PB84-152800

Totally Optical Technique for Monitoring Ambient Non-Methane Hydrocarbons

AeroChem Research Labs., Inc., Princeton, NJ

Prepared for

Environmental Sciences Research Lab.
Research Triangle Park, NC

Feb 84

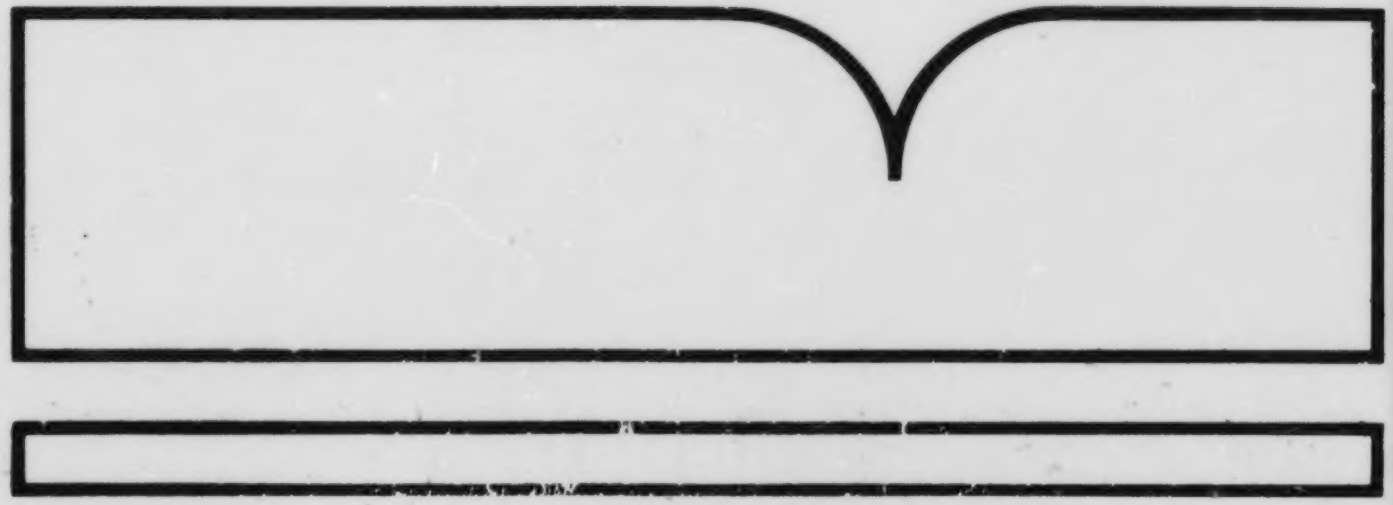

U.S. Department of Commerce
National Technical Information Service
NTIS

EPA-600/3-84-030
February 1984

TOTALLY OPTICAL TECHNIQUE FOR MONITORING AMBIENT NON-METHANE HYDROCARBONS

PB84-152800

by

Dennis M. Manos, Hermann N. Volltrauer,
and Jonathan Allen

AeroChem Research Laboratories, Inc.

Princeton, NJ 08540

and

Darrell E. Burch, John S. Chudy,
and John D. Pembrook

Ford Aerospace & Communications Corporation

AERONUTRONIC DIVISION

Newport Beach, CA 92660

Contract No. 68-02-3292

Project Officer

William McClenny
Atmospheric Chemistry and Physics Division
Environmental Sciences Research Laboratory
Research Triangle Park, North Carolina 27711

ENVIRONMENTAL SCIENCES RESEARCH LABORATORY
OFFICE OF RESEARCH AND DEVELOPMENT
U. S. ENVIRONMENTAL PROTECTION AGENCY
RESEARCH TRIANGLE PARK, NORTH CAROLINA 27711

REPRODUCED BY
NATIONAL TECHNICAL
INFORMATION SERVICE
U.S. DEPARTMENT OF COMMERCE
SPRINGFIELD, VA. 22161

TECHNICAL REPORT DATA
(Please read Instructions on the reverse before completing)

1. REPORT NO. EPA-600/3-84-030	2.
3. RECIPIENT'S ACCESSION NO. PB84 152800	
4. TITLE AND SUBTITLE TOTALLY OPTICAL TECHNIQUE FOR MONITORING AMBIENT NON-METHANE HYDROCARBONS	5. REPORT DATE February 1984
	6. PERFORMING ORGANIZATION CODE
7. AUTHOR(S) Dennis M. Manos, Hermann N. Volltrauer, and Jonathan Allen, and Darrell E. Burch, John S. Chudy, and John D. Pembrook	8. PERFORMING ORGANIZATION REPORT NO. AeroChem TP-423 Ford Aerospace U6743
9. PERFORMING ORGANIZATION NAME AND ADDRESS AeroChem Research Laboratory Inc. P.O. Box 12, Princeton, NJ 08540 and Ford Aerospace Communications Corp., Aeronutronic Div., Ford Rd., Newport Beach, CA 92663	10. PROGRAM ELEMENT NO. CDTA1D/01-0428 (FY-83)
	11. CONTRACT/GRANT NO. 68-02-3292
12. SPONSORING AGENCY NAME AND ADDRESS Environmental Sciences Research Laboratory-RTP, NC Office of Research and Development U.S. Environmental Protection Agency Research Triangle Park, NC 27711	13. TYPE OF REPORT AND PERIOD COVERED Final 9/79-9/82
	14. SPONSORING AGENCY CODE EPA/600/09
15. SUPPLEMENTARY NOTES	

16. ABSTRACT

A method for measuring ambient levels of nonmethane hydrocarbons (NMHCs) has been developed and an instrument based on that method has been built. The instrument consists of a sample conditioner and an optical CO_2-CO monitor. In the sample conditioner ambient air is scrubbed of CO_2 and H_2O and any NMHCs and CO present are catalytically oxidized to CO_2. The CO_2-CO monitor measures both the original CO present in the air as well as the CO_2 resulting from conversion of NMHCs and the CO. The CO_2 channel of the CO_2-CO monitor measures the concentration of the CO_2 produced, which is directly related to the concentration of NMHC. Carbon monoxide in the air is also oxidized to form CO_2; therefore, it is necessary to account for the amount of CO_2 produced by the oxidation of CO if the NMHC concentration is to be determined accurately. This is accomplished by using the CO channel of the monitor to measure the concentration of CO in the air before it passes through the oxidation stage. Circuitry incorporated in the analyzer produces linearized output signals of the CO and CO_2 concentrations as well as their difference, the concentration of carbon atoms in the NMHC.

17. KEY WORDS AND DOCUMENT ANALYSIS

a. DESCRIPTORS	b. IDENTIFIERS/OPEN ENDED TERMS	c. COSATI Field/Group

18. DISTRIBUTION STATEMENT RELEASE TO PUBLIC	19. SECURITY CLASS *(This Report)* UNCLASSIFIED	21. NO. OF PAGES 83
	20. SECURITY CLASS *(This page)* UNCLASSIFIED	22. PRICE

EPA Form 2220-1 (9-73)

NOTICE

This document has been reviewed in accordance with U.S. Environmental Protection Agency policy and approved for publication. Mention of trade names or commercial products does not constitute endorsement or recommendation for use.

BEGIN FIRST LINE OF TEXT HERE
TYPING GUIDE SHEET
CENTER OF PAGE
TOP OF IMAGE AREA
DROPPED HEAD BEGIN SECTIONS HERE

ABSTRACT

A method for measuring ambient levels of nonmethane hydrocarbons (NMHCs) has been developed and an instrument based on that method has been built. The instrument consists of a sample conditioner and optical CO_2-CO analyzer. In the sample conditioner ambient air is scrubbed of CO_2 and H_2O and any NMHCs and CO present are catalytically oxidized to CO_2. The CO_2-CO analyzer measures both the original CO present in the air as well as the CO_2 resulting from conversion of NMHCs and the CO. Circuitry incorporated in the analyzer produces linearized output signals of the CO and CO_2 concentrations as well as their difference, the NMHC concentration.

This report is submitted in fulfillment of Contract No. 68-02-3292 by AeroChem Research Laboratories, Inc. under the sponsorship of the U.S. Environmental Protection Agency. This report covers the full technical performance period from 28 September 1979 to 27 April 1982.

BEGIN LAST LINE OF TEXT HERE
BOTTOM OF IMAGE AREA OUTSIDE DIMENSION FOR TABLES AND ILLUSTRATIONS
3/8"

PAGE NUMBER
EPA-257 (Cont.) (4-76)

CONTENTS

Abstract iii

Figures vi

Tables vi

Acknowledgments vii

1. Introduction 1

2. Conclusions and Recommendations 2

3. Feasibility Study 3

A. Apparatus and Technique 3

1. Flow System 3

2. NDIR Monitors 6

B. Results and Discussion 6

1. Selective Oxidation of Hydrocarbons 6

2. Selective Removal of CO_2 10

3. CO Removal 13

4. Water Removal 16

C. Conclusions 17

4. Testing of the NMHC Converter 21

A. Perma Pure Dryer Tests 21

B. Tests of CO_2-CO Analyzer and Scrubber 23

References 25

Appendix A: Manual for a Monitor for CO_2 and CO

FIGURES

Number		Page
1.	Schematic of apparatus.	5
2.	HC conversion efficiency to CO_2 over hopcalite.	9
3.	Linearity test of hopcalite converter at low HC levels using ten component hydrocarbon mixture	10
4.	Schematic of two channel system	19
5.	Schematic of single channel system.	19
6.	Schematic of real time single channel system.	20
7.	Schematic of NMHC analyzer.	22
8.	Water removal efficiency of Perma Pure dryer.	23

TABLES

1.	HC Transmission of Hopcalite Catalytic Converter.	8
2.	HC Conversion to CO_2 on a Hopcalite Column at 580 K	8
3.	Hydrocarbon Transmission of Selective Scrubbers	12
4.	Percent of Initial CO Removed by Cu/Zn Catalyst at 530 K.	14
5.	Percent of Initial CO Removed by Cu/Cr Catalyst at 420 K.	14
6.	Percent HC or CO Removed by Cu/Zn Catalyst at τ_{res} = 0.75 s	14
7.	Modified Retardation Ratios, R, and Maximum HC Concentration as Percent of Maximum Through Blank	16

TYPING GUIDE SHEET

ACKNOWLEDGMENTS

R. Taweel and G. McComiskey performed the experimental work on this program. Dr. William McClenny of EPA made many helpful suggestions throughout the course of this work.

SECTION 1

INTRODUCTION

Ambient nonmethane hydrocarbons and nitrogen oxides (NO_x) are primary precursors of ozone and other oxidants, which are key components of photochemical smog. Current strategies for controlling these photochemical oxidants depend primarily on nonmethane hydrocarbon (NMHC) abatement. EPA has identified the development of improved monitoring techniques for NMHC as a basic need for the agency. In particular, the problem of response variability that is inherent in the measurement of the many molecular species comprising NMHCs must be addressed.

The goal of this work has been to develop and deliver a prototype instrument that measures NMHCs by optical absorption after converting each carbon atom in NMHCs to CO_2. The effort was preceded by a feasibility test to prove a design of a conditioner suitable for eliminating CO_2 from an ambient air sample and for converting NMHC quantitatively to CO_2 in a catalytic oxidizer. After feasibility was shown, the prototype monitor was built. This report provides the details of the feasibility study and limited performance testing of the instrument. The instrument itself is described in two manuals, one for the chemical converter[1] that converts the NMHC to CO_2 and the other for the optical CO_2-CO analyzer; the latter is included in this report as Appendix A.

---

1. Allen, J. and Volltrauer, H.N., "Manual for NMHC Converter," AeroChem TP-424, November 1982.

TYPING GUIDE SHEET
BEGIN FIRST LINE OF TEXT HERE
CENTER OF PAGE
TOP OF IMAGE AREA
DROPPED HEAD BEGIN SECTIONS HERE
BEGIN LAST LINE OF TEXT
BOTTOM OF IMAGE AREA OUTSIDE DIMENSION FOR TABLES AND ILLUSTRATIONS
3/8"
PAGE NUMBER
EPA 287 (Cin.) (4-76)

SECTION 2

CONCLUSIONS AND RECOMMENDATIONS

This work demonstrates that nonmethane hydrocarbons can be easily measured in real time by totally optical means. While complete testing of the total instrument was not possible, the testing that was carried out both in the feasibility study and with the completed instrument suggests that ambient levels of nonmethane hydrocarbons should be measurable.

Further work needs to be done--mainly thorough testing of the instrument including on site use.

SECTION 3

FEASIBILITY STUDY

The goal of the feasibility study was to find chemical scrubbers that would allow the real-time measurement of sub-ppm ambient levels of nonmethane hydrocarbons (NMHC) by optical techniques. Current methods of monitoring ambient levels of NMHC in air employ flame ionization monitors or hybrid devices which incorporate flame ionization with optical methods. The cost and inconvenience, especially for field measurements, of replacing the hydrogen and zero air used by such monitors makes the use of totally optical methods quite desirable.

In this work, we developed such a totally optical method. The strategy adopted was to convert the NMHC of interest quantitatively to CO_2 and then to measure the NMHC as CO_2 by using the high sensitivity and stability of nondispersive infrared (NDIR)[2] absorption. Technically, this requires the thorough removal of the ambient ($\approx$ 330 ppm) CO_2 in air and a method of compensating for the presence of CO in the ambient samples, since the CO is oxidized to CO_2 along with NMHC. Water, though always present in considerable concentration in ambient samples, is not a serious interferent ($<$ 3.6 ppb CO_2 interference per wt % of H_2O; private communication, D.E. Burch, 27 December 1979) in the NDIR measurement. Only enough water must be removed, therefore, to permit the effective operation of the scrubbers and converters. Finally, the NMHC converter itself must quantitatively convert all hydrocarbons except methane to CO_2.

A. Apparatus and Technique

1. Flow System

Preliminary tests were performed using an AeroChem ultrasensitive flame ionization monitor. This detector is sensitive to hydrocarbons (HCs) but not to CO_2, CO, or H_2O. These tests were aimed at determining which agents (scrubbers) remove the latter molecules while simultaneously transmitting HCs. The preliminary test apparatus included a gas feed system for delivery of fuel (H_2 zero gas). The hydrocarbon analyte was introduced through a metering valve into the oxidizer stream where it was diluted to an arbitrary level of interest (2-10 ppm). A pair of three-way valves allowed the

---

2. Herget, W.F., Jahnke, J.A., Burch, D.E., and Gryvnak, D.A., "Infrared Gas-Filter Correlation Instrument for in situ Measurement of Gaseous Pollutant Concentrations," Appl. Opt. 15, 1222 (1976).

diluted sample to pass through either a temperature controlled (297-700 K) scrubber column or a similar volume of empty tubing on the way to the monitor. A single flow rate ≈ 85 ml(STP)s^{-1} was used, yielding a residence time $\tau \approx$ 0.18 s in the scrubber columns. Measurements were made by flowing the oxidizer first with, then without analyte, through the blank column to establish the analyte concentration. The same procedure was then followed with the scrubber column. This gives the degree of loss of the HC on the scrubber. Adequate time (2-15 min) was allowed for reaching equilibrium on both columns and for establishing that the scrubber did not cause significant drift. The measurements alternated between scrubber and blank until each showed better than 1% reproducibility.

The main tests, employing the NDIR technique, were made with the more elaborate system shown in Fig. 1. The carrier gas (zero air) flows either through a water saturator or a bypass on its way to one inlet of a well-stirred dilution flask maintained at ≈ 360 K. Other flask inlets serve to admit samples either continuously, through a calibrated needle valve, or as (pulsed) injections of known volumes of prediluted samples through a septum. A mechanical pump provides rapid pumpdown and purging of the flask.

The continuous mode is useful in cases where dilution ratios < 100/1 are required. The pulsed injection mode[3] is useful where higher initial dilution ratios are required. By injecting volumes (10 µl to 100 ml) of various mixtures of analytes in air (12 ppm to 100% analyte), a wide range of analyte concentrations (sub-ppb to 5% analyte) may be produced.

The outlet of the dilution flask leads to a processing chain consisting of dryer, scrubber, and converter. The flow (2.5-100 ml(STP)s^{-1}) is controlled by a calibrated regulating valve and monitored by a calibrated rotameter. Each element of the chain may be bypassed through an approximately equal volume of empty tubing. The temperature of each element of the process chain is independently controlled.* In the continuous dilution mode the technique of investigating individual materials was identical to that used in the preliminary tests.

System calibration was checked using a standard CO_2 mixture and bypassing all scrubbers. For checking the pulsed mode, we compared the concentration vs. time profiles for injections through the scrubbers to those through the blanks. The temporal profiles of analyte concentration in the dilution flask were well-represented by an exponential decay[3] with a time constant determined by the flow rate and system volume. Each injection

---

3. Fontijn, A., "Chemiluminescence Techniques in Air Pollutant Monitoring," in Modern Fluorescence Spectroscopy, Vol. 1, E.L. Wehry, Ed. (Plenum Press, New York, 1976) p. 159.

* In cases where the Perma Pure dryer was used (see below) no provision was made to accurately control its temperature.

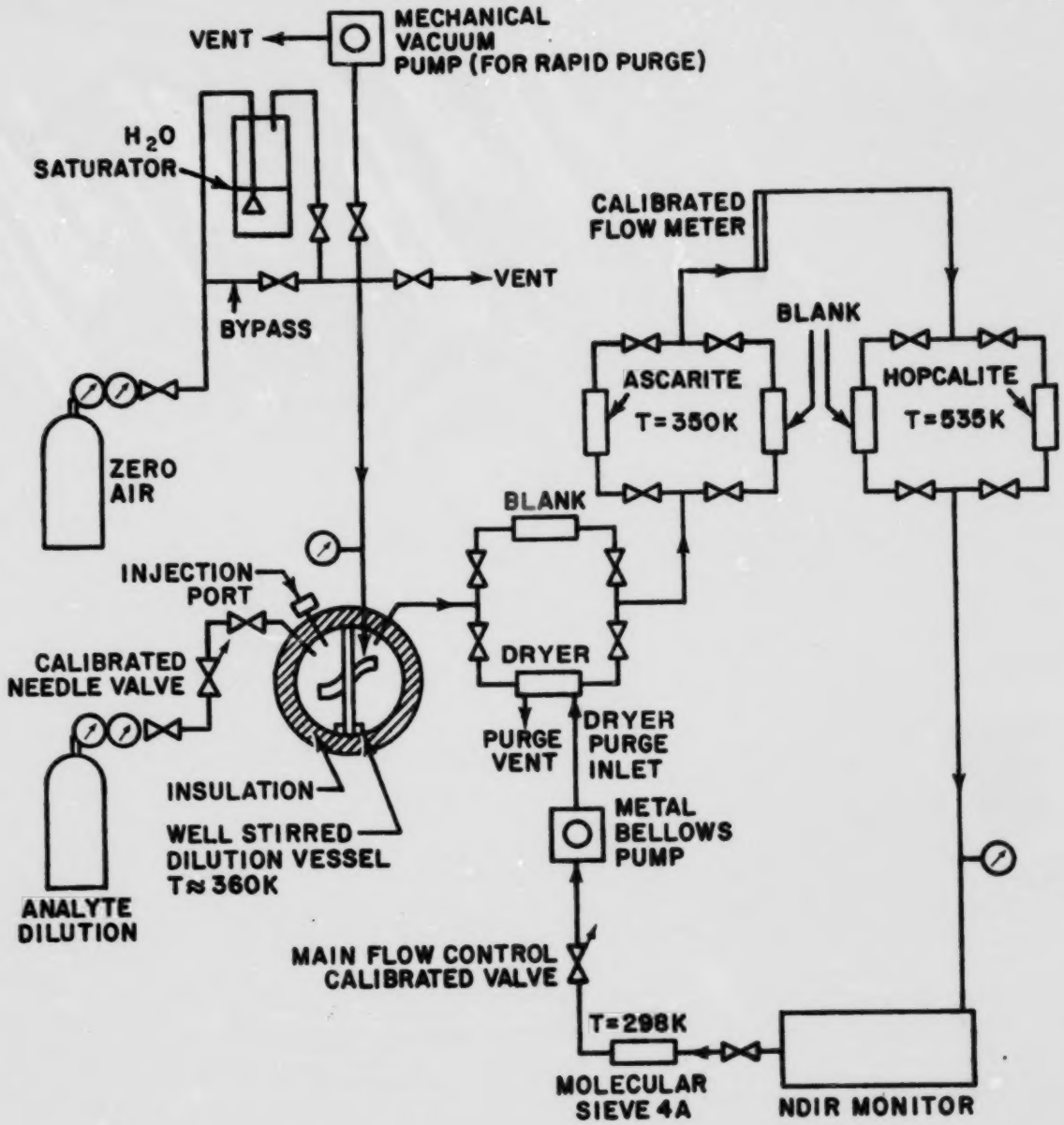

Figure 1. Schematic of apparatus.

therefore constitutes a continuous time series of measurements which may be quantitatively compared to the corresponding time series of the CO_2 calibration injection. The peak concentration values were reproducible between injections to within 5 to 10 percent.

2. NDIR Monitors

The breadboard nondispersive CO_2 monitor was built by Ford Aerospace Corporation for this work and we will not describe it in great detail here. It employs a rotating interference filter to view the 4.3 μm band of CO_2 absorption. By offering three choices of path length and five gain scales a wide range (0-200 ppm) of CO_2 concentrations was measurable; however, the instrument calibration was quite inaccurate beyond ≈ 50 ppm. The combination of short-term noise (noise equivalent concentration was ≈ 60 ppb) and drift limited the lower range of our studies to ≈ 100 ppb with this prototype instrument. Therefore lower limits reported here represent S/N between 1 and 2.

For detailed studies of selective oxidation of CO we used a CO monitor built by Ford Aerospace and lent to us by the EPA. The lower limit of CO concentration measurable using this instrument was ≈ 20 ppb.

B. Results and Discussion

1. Selective Oxidation of Hydrocarbons

In the preliminary flame ionization work we tested the transmission, as a function of temperature, of 2-10 ppm concentrations of ethane and hexane at ≈ 85 ml(STP)s^{-1} ($\tau \approx 0.18$ s) through a 15 cm x 1.25 cm diam cylinder filled with hopcalite (a proprietary material containing oxides of Cu and Ni). The results, expressed as the percentage of sample transmitted (Reading Through Converter ÷ Reading Through Blank) are given in Table 1. Between 540 and 590 K we found that all of the ethane was consumed (hexane is consumed completely at all temperatures tested) and we assumed that the consumption represented quantitative oxidation to CO_2 (i.e., one CO_2 produced per carbon atom consumed).

We verified this assumption by injecting dilute (150 ppb to 50 ppm) samples of various HCs through the hopcalite converter at 580 K and measuring the output CO_2* directly with NDIR at carrier flow rates from 15-50 ml(STP)s^{-1} (τ from 0.3 to 1.0 s). By comparing injected samples to CO_2, we may calculate the response of a particular sample as follows:

---

* CO_2 is recovered quantitatively after passing through hopcalite.

$$\kappa_{sample} = \frac{\left(\text{SAMPLE } CO_2 \text{ READING}\right)}{\left(\begin{matrix}\text{READING OF } CO_2 \\ \text{CALIBRATION} \\ \text{THROUGH BLANK}\end{matrix}\right)} \times \frac{\left(\begin{matrix}\text{INJECTED} \\ \text{VOLUME} \\ CO_2 \text{ CALIBRATION}\end{matrix}\right)}{\left(\begin{matrix}\text{INJECTED SAMPLE} \\ \text{VOLUME}\end{matrix}\right)}$$

$$\times \frac{\left(\begin{matrix}\text{CONCENTRATION OF} \\ CO_2 \text{ CALIBRATION}\end{matrix}\right)}{\left(\begin{matrix}\text{KNOWN CONCENTRATION} \\ \text{OF INJECTED SAMPLE}\end{matrix}\right)}$$

The results are shown in Table 2 expressed as the quantity, κ, the "response as CO_2" where the errors shown are the scatter of averaging the results. Clearly the relative response, within the error of the measurements, is equal to the number of carbon atoms in the analyte HC molecule, indicating that the consumption of the molecule represents complete oxidation to recoverable CO_2.

The small conversion of methane represents a problem for NMHC monitoring. We therefore investigated hopcalite selectivity as a function of temperature, measuring the % conversion to CO_2 for methane, ethane, propane, ethylene, acetylene, hexane, and butene. The results (for $\tau \approx 0.5$ s) are presented in Fig. 2, where 100% conversion represents a response of $\approx$ 1-2 ppm as CO_2 for NMHC and $\approx$ 10 ppm for methane. It can be seen that at 590 K, $\approx$ 10% of the methane would be converted to CO_2. The onset temperature for methane to CO_2 conversion was $\approx$ 535 K, where 0.8% of the methane was converted. At this temperature $\approx$ 96% of the ethane and 100% of all other hydrocarbons tested are converted to CO_2.

The manufacturer's literature[4] and one account of hopcalite use[5] suggest that methane should not be converted at temperatures below 540 K. It was therefore somewhat surprising to observe $\approx$ 1% conversion at this temperature. Poli and Zinn[6] reported the same troubling behavior in their studies using hopcalite. They attributed the problem to nonuniform heating which more careful design of the catalyst heater eliminated. In our apparatus we did not take much care to assure uniform heating so it is likely that this was responsible for the observed conversion. In designing an instrument using this catalyst it will be important to avoid such nonuniformity of temperature.

---

4. McDonough, J.B., "Detection, Reduction and Control of Gaseous Contaminants," Mine Safety Appliances, Filter Products Div. (1978).

5. "Methods of Air Sampling and Analysis," Intersociety Committee (American Public Health Association, Washington, DC 1972) p. 239.

6. Poli, A.A. and Zinn, T.L., "A New Continuous Monitor for Methane and Non-Methane Total Hydrocarbons," ISA AID 73431 (1973) p. 135.

TABLE 1. HC TRANSMISSION OF HOPCALITE CATALYTIC CONVERTER

Hopcalite[a] Column (15 cm x 1.25 cm diam)

Temperature (K)	% Transmission	
	Ethane	Hexane
310	81	0
330	80	0
380	83	0
460	62	0
490	23	0
540	4.0	0
590	0	0
690	0	0

[a] Mine Safety Appliances Part No. 21215, Mesh 6-14, Job No. 58768, date of manufacture 10/79, additional test data Lot 498. This material is not commercially available. Small quantities are sold to individuals at the discretion of MSA.

TABLE 2. HC CONVERSION TO CO_2 ON A HOPCALITE COLUMN AT 580 K

Sample	κ (response as CO_2)	No. of Carbon Atoms
CO_2	1.01 (± 0.05)	1
CO	1.02 (± 0.04)	1
Methane	0.07 (± 0.01)	1
Ethane	1.96 (± 0.07)	2
Ethylene	2.10 (± 0.10)	2
Acetylene	2.05 (± 0.10)	2
Propane	3.04 (± 0.12)	3
Butene	4.05 (± 0.20)	4
Hexane	6.01 (± 0.20)	6

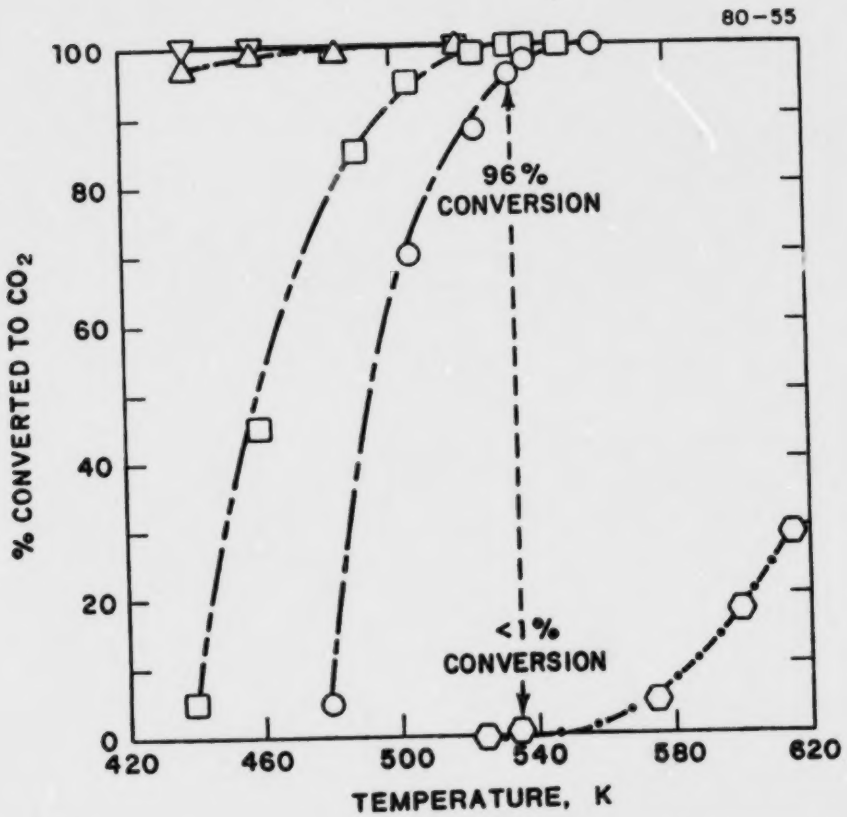

Figure 2. HC conversion efficiency to CO_2 over hopcalite. Residence time τ = 0.5 s. ⬡ - methane; ○ - ethane; □ - propane; - ethylene; ▽ - acetylene, butene, hexane.

Varying residence time from 0.10 s to ≈ 3 s did not produce any measurable response from CH_4 at 525 K. All compounds that were 100% converted at τ = 3 s were also 100% converted at τ = 0.1 s. Ethane conversion was constant from τ = 0.3 to 3 s but decreased by 2% as τ was decreased from 0.3 to 0.10 s. This suggests that a residence time of ≈ 0.35 s should be used in designing an instrument. Examining the HCs individually, complete conversion was found to be independent of concentration over the entire range accessible to our experiments (≈100 ppb to ≈ 50 ppm).

The possibility of synergistic effects among HCs at low concentration was also tested by analyzing a mixture of HCs in zero air. This mixture was composed of approximately equal parts (100 ppm) of methane, ethane, ethylene, acetylene, propane, propylene, hexane, hexene, xylene, and benzene, diluted with zero air and maintained in a cylinder at T ≈ 350-360 K to avoid adsorptive loss of high boiling components. The linearity of response demonstrated in Fig. 3 indicates that no synergistic effects occur. The total response is in direct proportion to the amount of carbon in the sample.

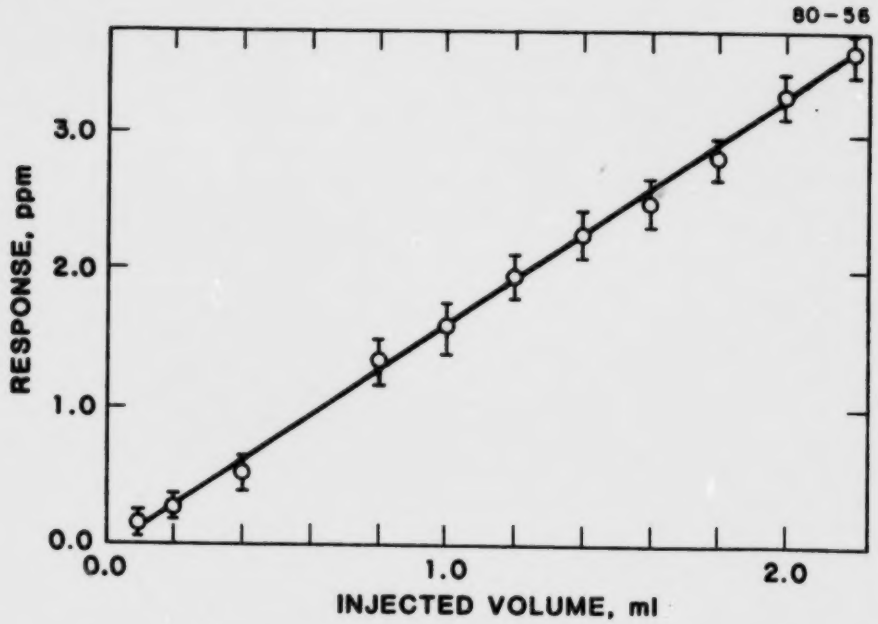

Figure 3. Linearity test of hopcalite converter at low HC levels using ten component hydrocarbon mixture.

T = 535 K; residence time $\tau \approx 0.5$ s.

2. Selective Removal of CO_2

The results of our preliminary tests of candidate CO_2 scrubbers are shown in Table 3. Based on these tests and previous experience with CO_2 removal, ascarite (alkaline metal hydroxide supported on an inert material, A.H. Thomas 60-80 mesh) was selected for more extensive study. A 15 cm x 1.25 cm diam column of ascarite maintained at $\approx$ 350 K was used for these tests. We found that at a flow rate of 5 ml(STP)s^{-1} ($\tau \approx 3$ s), transient concentrations of up to 5% V/V CO_2 were not detectable after passage through this scrubber. A steady flow of $\approx$ 400 ppm CO_2 at 80 ml(STP)s^{-1} was monitored for 20 h* through a 25 g fresh ascarite column, and again no CO_2 was detectable. At the end of this period, multiple injections of 5000 ppm at 50 ml(STP)s^{-1} showed that this ascarite had not suffered any diminution in ability to handle high transient CO_2 levels. The indicator in the ascarite showed some color change; however, the ascarite itself was still serviceable (its limit of uptake is 20-30% by weight). Based on our results, we expect a lifetime of ≥ 1 day g^{-1} of ascarite for scrubbing ambient levels at flows of 200 ml(STP) min^{-1}.

---

* Equivalent to more than three weeks of continuous scrubber operation of $\approx$ 350 ppm ambient CO at 200 ml min^{-1}.

The transmission of HC through the ascarite scrubber was tested. The signal due to the HC mixture did not change (100% ± 5%) over the range used in the hopcalite linearity (above) test (150 ppb-3.5 ppm) after passing through ascarite ($T \approx 350$ K) at $\tau = 0.3$-0.75 s. Individual HCs, including ethane, propane, butane, butene, hexane, and benzene, were tested over a range of flows (3-100 ml(STP)s^{-1}) and concentrations (0.25-50 ppm). All were nearly quantitatively transmitted. It is known[7] however, that alcohols, aldehydes, and ketones will not be transmitted through alkaline materials such as ascarite. None of these compounds was tested.

The response of ascarite to CO was also tested. A fresh ascarite column was used to determine the transmission of CO at flows from 5-50 ml(STP)s^{-1} ($\tau \approx 0.3$-3 s). The results of these tests showed that > 99% (± 5% error for averaging) of the CO is transmitted, indicating that there is no discernable initial CO uptake. This same ascarite was then subjected to a 2 ml(STP)s^{-1} flow of pure CO for 8 h with no visible color change of the indicator. The column was then briefly (≈1 min) purged with zero air and the above transmission tests repeated with the same results. Comparison of the temporal decay of CO through the blank column and through the ascarite indicates that ≈ 100% transmission occurs down to the limits of measurement (≈ 100 ppb).

We note that the performance of ascarite is greatly impaired by the presence of high concentrations of water. The material channels* quite readily when exposed to moist air (saturated at 293 K). A 20 g sample was completely destroyed, caking into a solid mass, by less than 4 h exposure at 80 ml(STP)s^{-1} to such a moist air stream.

---

7. Karels, G.G. and Vincent, R.C., "Continuous Method for Sampling Stack Gases for Total Carbon," Env. Sci. Techn. 12, 1046 (1978).

* Channeling is defined as the creation of paths (or channels) in the material through which the gas may flow rapidly, having only little contact with the scrubber material. This was indicated by a sudden rise in CO_2 reading which could be rapidly reversed by tapping the column a few times.

TABLE 3. HYDROCARBON TRANSMISSION OF SELECTIVE SCRUBBERS

Material	Temp. (K)	% Transmission	
		Ethane	Hexane
Drierite	297	82	100
Silica Gel	297	78	0
Silica Gel	350	86	---[a]
Linde-3A	297	75	98
Linde-3A	350	81	100
Linde-3A	400	82	100
Davison-3A	297	79	98
Davison-3A	350	79	98
Davison-4A	297	68	79
Davison-4A	350	76	96
Coast-5A	297	100	100
Davison-5A	297	77	99+
Davison-5A	350	76	< 1
Linde-13X	297	77	0
Davison-13X	297	85	0
Carbowax 400 on Chromosorb-P	297	100	100
Carbowax 400 on Chromosorb-W	297	86	100
Carbowax 400 on Chromosorb-W	365	89	100
Carbowax 400 on Activated Alumina	297	76	100
Ascarite	297	78	100
Ascarite	365	86	95
Soda-Lime	297	90	100
Soda-Lime	350	75	100
Soda-Lime	400	86	100
50% Ascarite/50% Soda-Lime	350	85	100
50% Ascarite/50% Soda-Lime	400	80	100
Activated Charcoal	297	87[b]	0
Activated Charcoal	350	80	0
Copper Chrome on Carbon	297	80	0
Copper Chrome on Carbon	400	86	0

TABLE 3. (Continued)

Material	Temp. (K)	% Transmission	
		Ethane	Hexane
Copper Zinc on Alumina	297	87	93
Copper Zinc on Alumina	450	85	100
Copper Zinc on Alumina	500	94	100
Copper Zinc on Alumina	550	85	100
Copper Zinc on Alumina	600	88	73
Copper Chrome Tablets	297	77	85
Copper Chrome Tablets	450	85	93
Copper Chrome Tablets	500	86	56

[a] Would not equilibrate, continuous rise for > 30 min.

[b] Final reading took 3 min to achieve.

3. CO Removal

Our efforts to find a selective scrubber for CO were not successful. Instead, an alternate method for accounting for CO was developed (see below). Preliminary tests had identified two candidate CO scrubbers (supplied by W.R. Grace) both of which are proprietary catalysts. One contains Cu and Zn, partly as oxides in an exchanged zeolite support, the other Cu and Cr, also partly as oxides in a zeolite support.

For the tests of CO removal we bypassed the hopcalite and employed the NDIR CO monitor provided by the EPA. As shown in Tables 4 and 5 the effectiveness of these catalysts at removing CO quantitatively was excellent. However, tests with the HC mixture quickly indicated that considerable amounts of HCs were being lost in these CO scrubbers in spite of the mild catalytic activity of Zn and ZnO and the reported strong specific affinity[8] of CO for CuO. We performed more extensive tests using individual hydrocarbons, varying the temperature of the catalyst bed at $\tau = 0.75$ s. These results for the Cu/Zn catalyst are shown in Table 6. No temperature could be found where CO could be selectively removed by the Cu/Zn catalyst. Tests with the Cu/Cr catalyst yielded similar results.

---

8. Sergeys, F.J., Maher, P.K., Briggs, W.S., and McDaniel, C.V., "Method of Treating Exhaust Gases," U.S. Patent 3,346,328, 10 October 1967.

TABLE 4. PERCENT OF INITIAL CO REMOVED BY Cu/Zn CATALYST AT 530 K

τ Residence Time (s)	Initial CO = 2 ppm	Initial CO = 25 ppm	Initial CO = 75 ppm
0.15	96	96	---
0.25	100	98	89
0.33	100	98.5	96
0.75	---	100	100
2.0	---	100	100

TABLE 5. PERCENT OF INITIAL CO REMOVED BY Cu/Cr CATALYST AT 420 K

τ Residence Time (s)	Initial CO = 7.5 ppm	Initial CO = 75 ppm	Initial CO = 175 ppm
0.25	94	90	---
0.33	97	95	90
0.75	100	99.3	98

TABLE 6. PERCENT HC OR CO REMOVED BY Cu/Zn CATALYST AT τ_{res} = 0.75 s

T (K)	CO	Ethane	Acetylene	Ethylene	Propane	Butene	Benzene
295	0	-	-	-	-	-	-
325	0	-	-	-	-	-	-
375	0	-	51	0	-	-	-
425	30	0	82	5	0	57	0
450	91	0	92	7	0	65	0
485	100	0	100	13	0	68	0
525	100	0	100	98	< 1	70	0

At this point search for a selective, quantitative scrubber for CO was discontinued in favor of a method for dealing with ambient CO by measuring and correcting for its presence. In this method the NMHCs are selectively delayed and only CO is passed rapidly. This CO is converted to CO_2 and thus a measurement of CO is obtained. This value is then subtracted from the measured (NMHC + CO) obtained from the ascarite-hopcalite flow chain. To separate CO we prepared columns of activated charcoal in a 1.25 cm diam tube in lengths of 15 to 60 cm and investigated the transmission of low levels of CO (0.2 to 2 ppm) and high levels (5-50 ppm) of various HCs. In every test CO transited the charcoal in approximately the same period of time required to transit the blank column, yielding temporal profiles which were not distinguishable within the limits of the measurement. In sharp contrast, HCs injected through the charcoal were "held up" for variable periods of time until they began a gradual rise to some fraction of the value associated with the same size injection into the blank column. We define a modified* retardation ratio

$$R = \frac{T_{RC} - T_{RB}}{T_{RB}}$$

where T_{RC} is the elapsed time from the HC injection into the charcoal to the beginning (obtained by back extrapolating the rise curve) of the rise in signal. T_{RB} is the time to the peak of the signal caused by an identical HC injection through a blank of equal volume. The modified retardation ratio as defined above is relatively independent of column length and flow. Table 7 shows the values of R observed for various hydrocarbons on room temperature charcoal, charcoal at 273 K, and room temperature silica gel. As anticipated from literature reports of such columns,[10,11] the length of time these columns may be used for CO measurement before backflushing (purging with a reverse flow of HC-free gas) is required, is limited by ethane, acetylene, and ethylene. These HCs transit the charcoal fastest and ultimately rise to a high percentage of their initial concentrations.

---

* Normally the retardation ratio would be defined with T_{RC} being the elapsed time to the peak concentration observed through the column.[9]

9. Keulemans, A.I.M., Gas Chromatography, 2nd ed. (Reinhold, New York, 1959) p. 145.

10. Innes, W.B. and Andreatch, A.J., "Hydrocarbon and Carbon Monoxide Analysis by the Selective Combustion Method," Env. Sci. Techn. 4, 143 (1970).

11. Ortman, G.C., "Monitoring Methane in Atmosphere with a Flame Ionization Detector," Anal. Chem. 38, 644 (1966).

TABLE 7. MODIFIED RETARDATION RATIOS, R, AND MAXIMUM HC CONCENTRATION AS PERCENT OF MAXIMUM THROUGH BLANK

	Activated Charcoal T = 298 K		Activated Charcoal T = 273 K		Silica Gel T = 298 K	
	R	Max %	R	Max %	R	Max %
CO	0	100	0	100	0	100
Ethane	400	80	500	70		
Ethylene	480	25	680	15	250	56
Acetylene	280	42	520	23	240	80
Propane	470	2	470	1.3	360	35
Propylene	300	0.9	760	0.5		
Butane	300	0.2	300	0.1		
Butene	300	0.6	400	0.1	>1000	0
Hexane	>2400	0	>2400	0		
Toluene	>2400	0	>2400	0		
Benzene	>2400	0	>2400	0	>1000	0

These results indicate that conservative design would limit the useful period to $\approx$ 300 times the transit time before backflushing of a room temperature column in order to minimize interference from ethane, acetylene, and ethylene. Cooling to 273 K would extend this factor to $\gtrsim$ 400. Thus reasonable periods of use ($\approx$1 h) should be easily achieved before purging is required.

4. Water Removal

The CO monitor borrowed from EPA also measured H_2O in the 0-5% range with an estimated sensitivity of $\lesssim$ 500 ppm. We used this H_2O channel to test the drying capacity of a 5A molecular sieve (Coast Engineering, 60-80 mesh). At T $\approx$ 370 K, τ = 0.3 s, the 5A sieve (15 cm column, 1.25 cm diam) dried room temperature air containing 2-3% H_2O to below the 500 ppm level.

Hydrocarbon transmission through the 5A sieve was tested with the HC mixture. Complete transmission was observed with dry air, for HC concentrations of $\approx$ 150 ppb to 5 ppm at τ = 0.3-1.0 s. To test synergistic effects with water, we pulse-injected samples of the HC mixture into dry carrier gas flowing through the 5A sieve at T = 370 K. During the smooth decay of these pulses, sufficient water was injected into the dilution flask (T $\approx$ 360 K) to saturate the dry air carrier. No perturbation of the smooth decay was observed at any HC concentration tested (0.5-5 ppm). Similar tests with CO showed that the 5A sieve transmits 100% of CO at 200 ppb-5 ppm, τ = 0.15 to 1.0 s in wet (saturated at $\approx$ 365 K) or dry air.

The primary disadvantage of the 5A molecular sieve is that a large volume of material must be used in order to achieve an adequate lifetime of such a dryer. This adds considerably to the response time. We therefore tested a Perma Pure Products regenerative dryer. As shown in Fig. 1 the Perma Pure dryer is continuously flushed with a counterflow of dry gas. The manufacturer[12] indicates that optimum drying occurs with the use of a counterflow of 1.5 times the sample flow. We found that simply using (for the counterflow) the main flow after passing through a large dryer containing molecular sieve 4A, gave adequate drying performance to avoid damage to the ascarite even when continuously flowing H_2O saturated air at 298 K. We tested hydrocarbon transmission in the same manner as done for the 5A, first by comparing the dryer to a blank using dry air, then by injecting H_2O into samples of the mixture while passing through the dryer. Similar tests were performed using CO. Using the Perma Pure dryer we saw 100% transmission of both CO and the hydrocarbon mixture (for 200 ppb-5 ppm, τ = 0.2-0.7 s) and no interference from H_2O. It is likely that the use of a heated sample stream kept the membrane from adsorbing hydrocarbons in our tests. (This would seem to be even more important for dry samples where the membrane would be easily wetted by less volatile components of the mixture.) We did not attempt to measure the dryer temperature. It is quite likely that it was considerably above room temperature since the length of 1/4 in. tubing separating the dryer and the hot dilution flask (365 K) was short ($\lesssim$ 10 cm) and the flow rates were fairly high (5-100 ml(STP)s^{-1}). With comparable preheating of ambient samples, a Perma Pure dryer should prove useful in monitor applications. We note that, like ascarite, this device will not transmit some alcohols, aldehydes, and ketones.

C. Conclusions

Our studies have shown that hopcalite can be used to provide selective conversion of nonmethane hydrocarbons to provide a linear response as CO_2 from $\approx$ 100 ppb to $\approx$ 50 ppm, the limits dictated by the capabilities of the NDIR detector. Using heated (T $\approx$ 535 K) hopcalite, > 96% of ethane and 100% of CO can be converted quantitatively to CO_2 while converting a negligible (< 1%) fraction of methane. The major known poison for this catalyst[4] is H_2O, which only reduces the activity toward CO oxidation at temperatures below 373 K and hence is not a threat in this application.

Ascarite effectively reduces ambient levels of CO_2 to less than detectable limits (in this study < 100 ppb) and will do so with an estimated effective lifetime of $\approx$ 1 day g^{-1} of ascarite at flow levels anticipated in a working instrument. Ascarite is capable of scrubbing transient CO_2 levels far in excess of the ambient $\approx$ 350 ppm even after long periods of use. However, it is very hygroscopic even at $\approx$ 325 K, and hence is destroyed by prolonged exposure to wet sample streams. Ascarite at $\approx$ 325 K quantitatively transmits CO and all hydrocarbons tested.

---

12. Kertzmann, J., "Continuous Drying of Process Sample Streams," ISA AID 73425, 121 (1973).

The reduction of the lifetime of the ascarite in wet air is the principal reason that some degree of sample drying is required. For this purpose we have found two dryers which provide adequate dehydration while quantitatively transmitting CO and all hydrocarbons tested: Molecular sieve 5A at ≈ 375 K and the Perma Pure Products continuous regenerative dryer operated near 320 K.*

A selective, quantitative scrubber for CO was not found. Therefore, we must measure NMHC + CO and independently determine the CO background for subtraction. There are two distinct methods to perform this task, shown schematically in Figs. 4 and 5. The first, Fig. 4, would use two NDIR monitoring channels, one for measuring CO and the other for NMHC + CO.† (A variation of this, shown in Fig. 6, was considered in Phase II of this work - see below.) The sample would be split after the scrubber train, and one fraction sent to the CO channel to give a direct measure of the ambient level of CO‡ and the other fraction sent to the hopcalite column for oxidation before entering the CO_2 detector. The latter processing thus gives NMHC + CO. Because of its simplicity and reliability and because it provides truly continuous ambient monitoring of both NMHC and CO it is strongly to be preferred over the alternative approach shown in Fig. 5. (For purposes of discussion the valves drawn schematically are all two-way. In actual practice, of course, multiport valves would be used.)

In the second method (Fig. 5) the sample is split after passing through the ascarite. One portion is routed directly to the hopcalite and then to the CO_2 instrument for measurement of NMHC + CO. The other portion is routed to a parallel arrangement of two (or possibly more) columns containing activated charcoal. The timing sequence would be such that for half of a measurement period the flow would be through the NMHC + CO arm and for the second half of this measurement period the flow would be through one of the charcoal columns of the CO arm (which can easily be maintained at a temperature ≦ 0°C thermoelectrically although such a low temperature would not be necessary). The flow from the outlet of the CO_2 monitor, essentially clean, dry, zero air containing traces of methane, would be used to backflush the other charcoal column (which may be heated during this time by reversing the current in its thermoelectric cooler). This sequence would be repeated until the total exposure time of the charcoal column in use in the CO arm was ≈ 300-400 times the carrier transit time (perhaps ≈ 1-2 h). At the end of that period the other charcoal column would be cooled and brought into service and the first would be warmed and backflushed. If only two columns were used the total time of backflushing would be about twice the total time of exposure to the forward sample flow.

---

* Later tests showed this temperature to be too high (see Section 4.A).

† This two channel system was ultimately selected by EPA.

‡ All of the members of the processing train have been shown to transmit CO quantitatively.

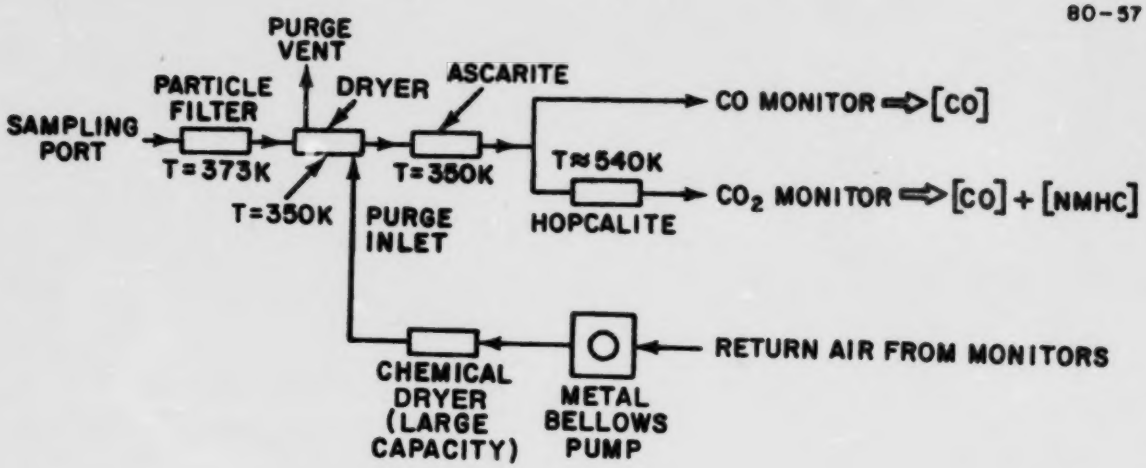

Figure 4. Schematic of two channel system.

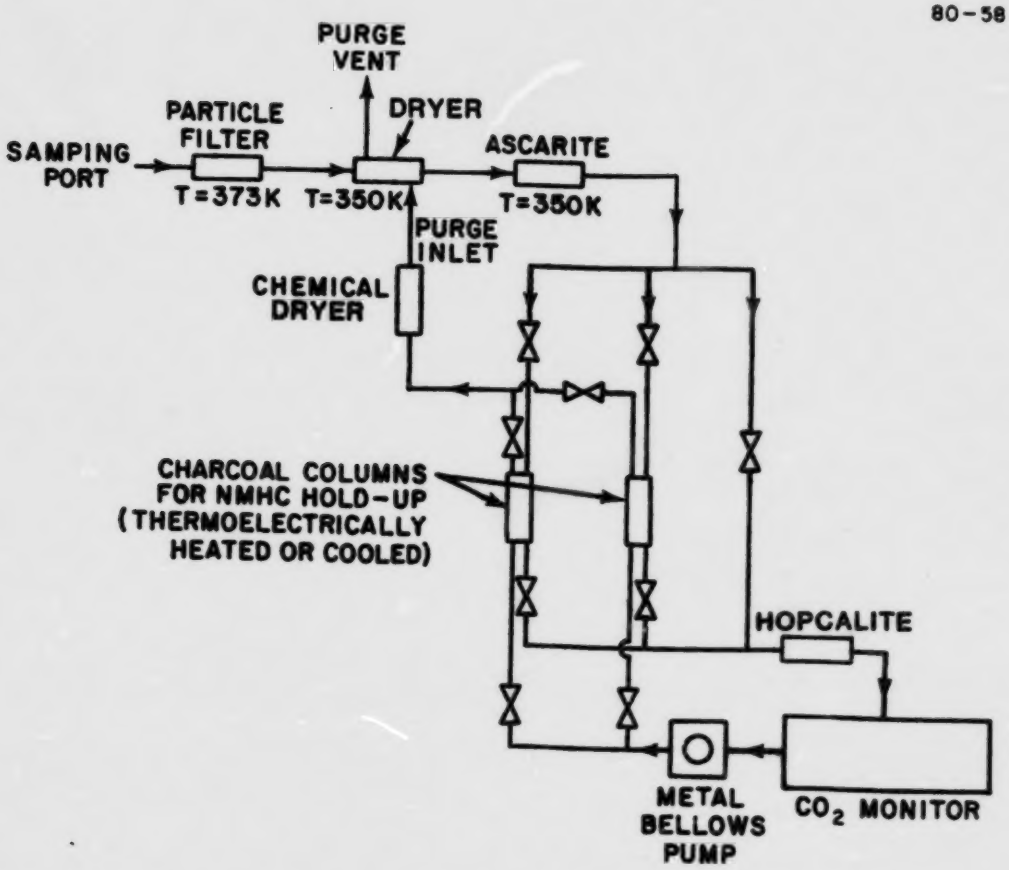

Figure 5. Schematic of single channel system.

This approach has the advantage of requiring only one NDIR channel. However, it is far more complex than the one outlined above and offers a much increased prospect of mechanical or electrical failure. In addition, it provides only an intermittent measurement of NMHC and CO and hence will miss some of the potentially interesting transients which may be seen with a continuous monitor. Because of its complexity this one cell approach was not chosen.

Another one cell approach was considered, however, in the second phase of this work. A schematic of this arrangement in which a single cell would be used to measure both CO and CO_2 in real time, is shown in Fig. 6. This approach would require precise flow control since two flows are mixed and any error in relative flows would show up as an error in concentration.

Precise flow control is also required in the two cell approach chosen (Fig. 4) but for different reasons. Flows in this case are matched to the sample cell volumes so as to achieve equal response times for the two channels. Changes in one flow relative to the other will thus cause a delay in one reading relative to the other and can cause errors in HC concentrations if CO concentrations change rapidly.

80-114

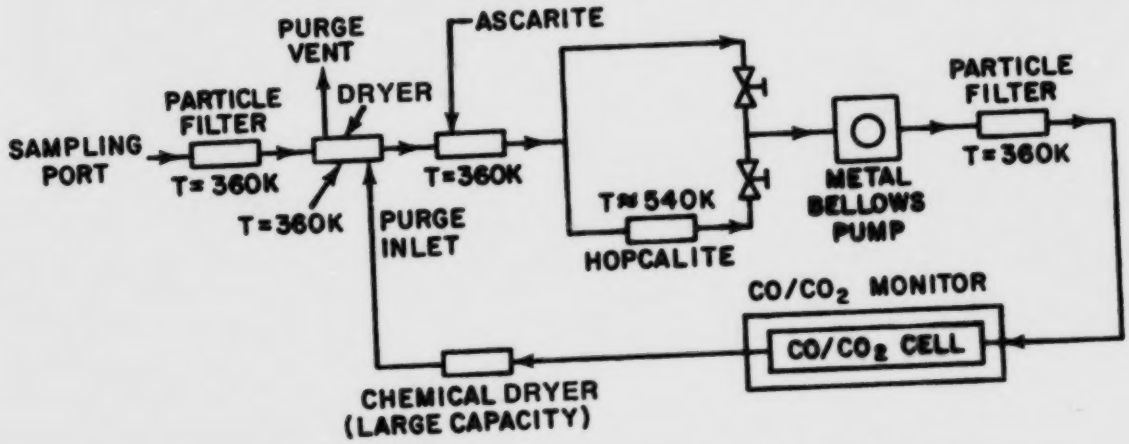

Figure 6. Schematic of real time single channel system.

SECTION 4

TESTING OF THE NMHC CONVERTER

Testing of the NMHC converter (sampler conditioner) was limited by continual malfunctioning of the optical CO_2-CO analyzer. The CO_2-CO analyzer problems were twofold: (1) a gas leak in the optical compartment made the background (zero) of the instrument strongly dependent on the flow rate of flush gas through that compartment and (2) a continuous loss in sensitivity made it impossible to attain low level measurements and to obtain reproducible results. These two problems have been corrected but time limitations prevented us from repeating tests with the repaired instrument. The tests that were carried out consisted mainly of determining the efficiency of the Perma Pure dryer and of determining the response of the instrument towards CO_2 and ethane. Figure 7 is a schematic representation of the complete instrument (see Ref. 1 and Appendix A).

A. Perma Pure Dryer Tests

The original intent (see Section 3.C) was to operate the Perma Pure dryer at near 325 K so that it would readily pass hydrocarbons. With the dryer at that temperature, however, its water removal efficiency was so poor that the ascarite (strong base) scrubber that is used to remove CO_2 and which was originally placed downstream of the Perma Pure dryer quickly clogged and became useless. This problem was shown to be due to a decrease in efficiency of the Perma Pure dryer with increasing temperature. Separate tests performed with the dryer, in which the water content of the air passing through it was measured, revealed the strong temperature dependence of its drying efficiency. To measure water concentration in air, we made use of the variation in ozone output of our discharge ozonator with water content of the air passing through it. The ozonator was calibrated from an air supply of known water content (a condenser at a fixed temperature). Results of a test in which 10 ml s^{-1} of air with a 3% water content was passed into the Perma Pure dryer as its temperature was varied are shown in Fig. 8 as % water removal efficiency. As can be seen from the figure the efficiency of the dryer is only 60% at 325 K but remains as high as 80% up to about 310 K. This is still significantly lower than expected. Because of the indirect method of testing, these efficiencies are uncertain by 10-15% although the relative values are probably precise to $\approx$ 5%. As a result of this test we decided that it would be necessary to run the Perma Pure dryer near ambient temperatures.

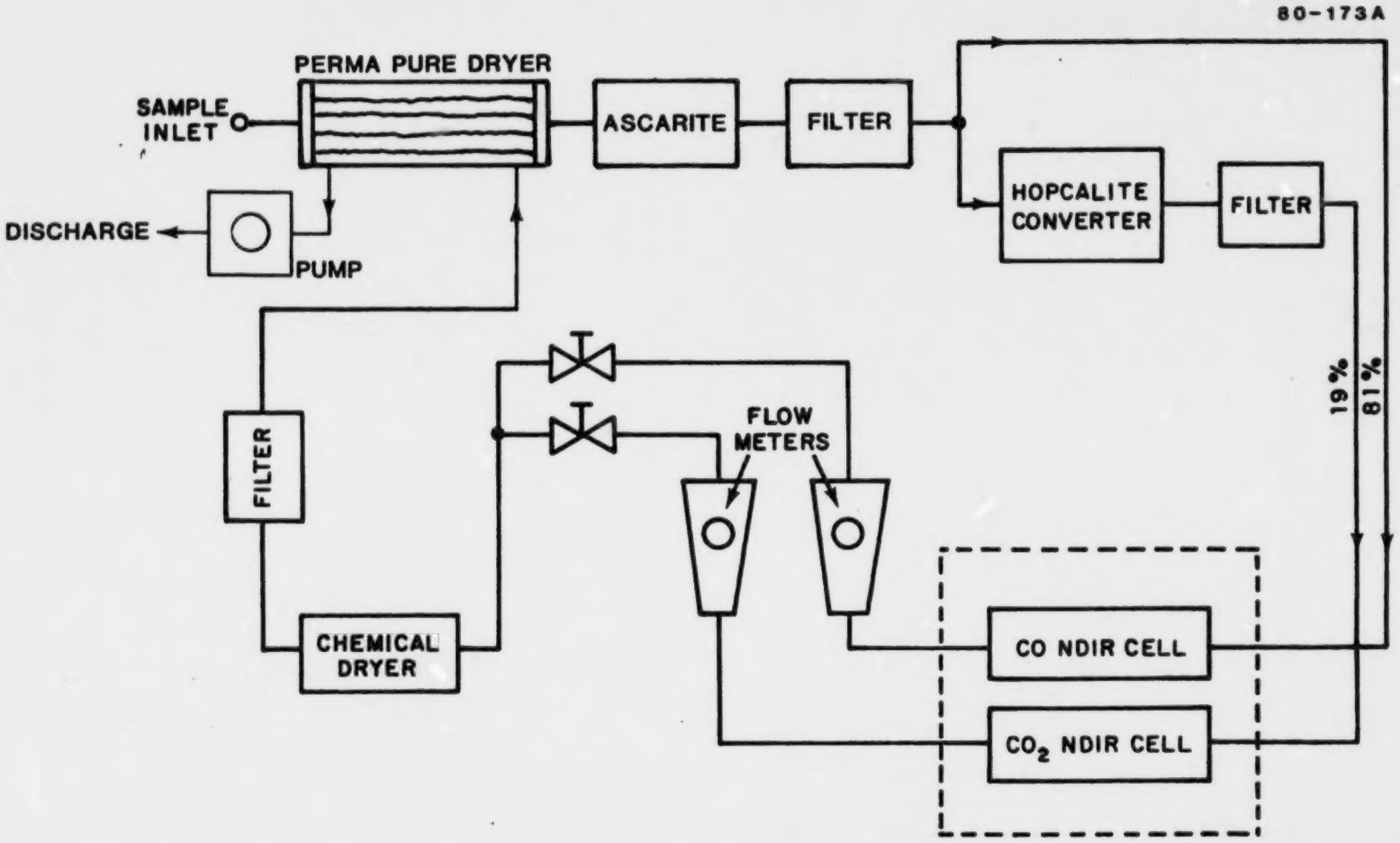

Figure 7. Schematic of NMHC analyzer.

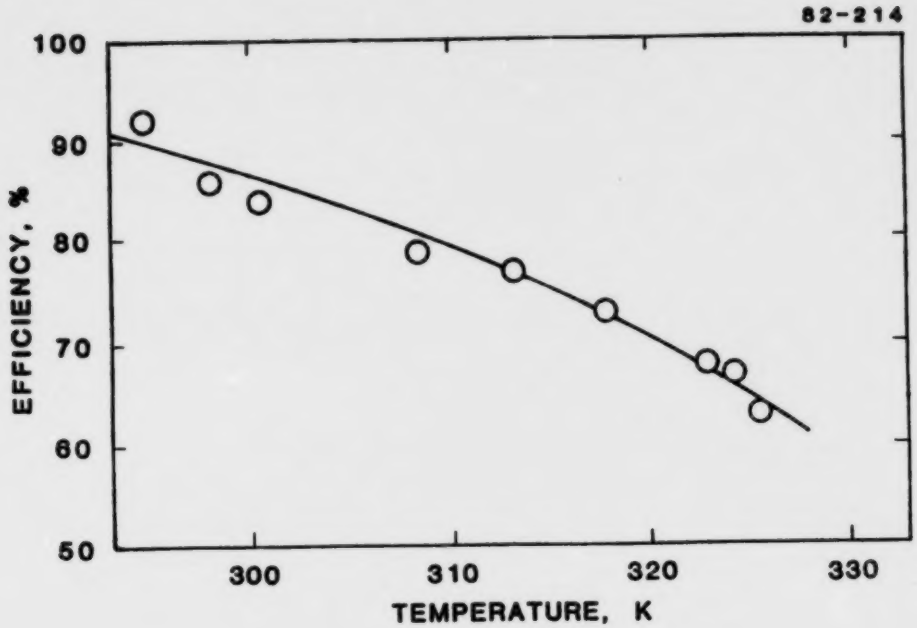

Figure 8. Water removal efficiency of Perma Pure dryer. Flow rate: 10 ml s^{-1} of 3% water content air.

B. Tests of CO_2-CO Analyzer and Scrubber

The planned initial tests of the CO_2-CO analyzer were to be determinations of zero and span stability. A low flow, about 2 ml s^{-1}, of nitrogen was passed into the purge inlet of the analyzer. This flow prevents ambient air (which can have varying amounts of CO_2) from entering the optical paths inside the instrument. Small changes in this purge gas flow rate had large effects on the zero reading of the instrument: the higher the purge flow, the lower the zero reading. At a 2 ml s^{-1} purge flow rate a 600 ppb higher reading was obtained than at a 17 ml s^{-1} purge flow and at 2 ml s^{-1} purge flow the zero changed at a rate of about 75 ppb for each ml s^{-1} change in purge flow rate. By maintaining a high purge flow rate relatively stable zero readings could, however, be maintained. This problem was later traced to a leak in the compartment containing the optics and has been corrected.

A more serious problem developed immediately on testing CO_2 and hydrocarbons. For these tests, air was passed through a 3.3 L heated exponential dilution flask and small amounts of CO_2 and ethane were injected into the flask. Initially both CO_2 and ethane gave the expected responses (ethane twice that of CO_2). However, over a course of a few weeks, readings continuously decreased for the same amount of injected CO_2 until only about a tenth of the original sensitivity was obtained. Later inspection by Ford Aerospace personnel indicated the problem to be due to an oil film on the mirrors and this problem was corrected.

Because the time available for testing of the completed instrument was used to determine and to try to circumvent the problems of the optical module, no further tests could be carried out.

REFERENCES

1. Allen, J. and Volltrauer, H.N., "Manual for NMHC Converter," AeroChem TP-424, November 1982.

2. Herget, W.F., Jahnke, J.A., Burch, D.E., and Gryvnak, D.A., "Infrared Gas-Filter Correlation Instrument for in situ Measurement of Gaseous Pollutant Concentrations," Appl. Opt. 15, 1222 (1976).

3. Fontijn, A., "Chemiluminescence Techniques in Air Pollutant Monitoring," in Modern Fluorescence Spectroscopy, Vol. 1, E.L. Wehry, Ed. (Plenum Press, New York, 1976) p. 159.

4. McDonough, J.B., "Detection, Reduction and Control of Gaseous Contaminants," Mine Safety Appliances, Filter Products Div. (1978).

5. "Methods of Air Sampling and Analysis," Intersociety Committee (American Public Health Association, Washington, DC, 1972) p. 239.

6. Poli, A.A. and Zinn, T.L., "A New Continuous Monitor for Methane and Non-Methane Total Hydrocarbons," ISA AID 73431 (1973) p. 135.

7. Karels, G.G. and Vincent, R.C., "Continuous Method for Sampling Stack Gases for Total Carbon," Env. Sci. Techn. 12, 1046 (1978).

8. Sergeys, F.J., Maher, P.K., Briggs, W.S., and McDaniel, C.V., "Method of Treating Exhaust Gases," U.S. Patent 3,346,328, 10 October 1967.

9. Keulemans, A.I.M., Gas Chromatography, 2nd ed. (Reinhold, New York, 1959) p. 145.

10. Innes, W.B. and Andreatch, A.J., "Hydrocarbon and Carbon Monoxide Analysis by the Selective Combustion Method," Env. Sci. Techn. 4, 143 (1970).

11. Ortman, G.C., "Monitoring Methane in Atmosphere with a Flame Ionization Detector," Anal. Chem. 38, 644 (1966).

12. Kertzmann, J., "Continuous Drying of Process Sample Streams," ISA AID 73425, 121 (1973).

APPENDIX A

Contract Number 68-02-3292(J167)

Ford Aerospace & Communications Corporation
Aeronutronic Division
Newport Beach, California 92660

MANUAL FOR A MONITOR FOR CO_2 AND CO

by

Darrell E. Burch, John S. Chudy, and John D. Pembrook

U. S. Environmental Protection Agency
Office of Research and Development
Environmental Sciences Research Laboratory
Research Triangle Park, North Carolina 27711

NOTICE

This document has been reviewed in accordance with U.S. Environmental Protection Agency policy and approved for publication. Mention of trade names or commercial products does not constitute endorsement or recommendation for use.

FIGURES

Number		Page
1	Optical diagram of the source optics	4
2	Optical diagram of the multiple-pass optics in the CO_2 sample cell	6
3	Image patterns on mirrors S4 of the CO_2 and CO sample cells	7
4	Block diagram of the electronics used to process the detector signals	11
5	Calibration curves relating the CO_2 concentration to the analog output signal of the optics assembly	15
6	Calibration curves relating the CO concentration to the analog output signal of the optics assembly	16
7	Mounting brackets for the optics assembly	19
8	Electrical power distribution circuits	28
9	Locations of heating resistors and thermocouples . . .	29
10	Circuit diagram of the main electronics card	34
11	Main Electronics Card Assembly	37
12	Circuit Diagram of the 30 Hz Reference Card	38
13	Detector Preamplifier Circuit Diagram and Assembly . .	39
14	Circuit Diagram of the Range Card	40
15	Simplified block diagram of the Digital Processor . . .	43
16	Electrical interface between Optical Assembly and Data Processor	44
17	Data Processor Flow Chart	45

34<

CONTENTS

Section		Page
Figures	. . . . .	iii
1	Introduction and Summary	1
2	Layout of Optical Assembly	3
	GFC and Entrance Optics	3
	Sample Cells and Detectors	5
3	Principles of Operation of Optical Assembly	9
	GFC and Principles of Detection	9
	Electronics and Processing of Detector Signals . . .	10
4	Calibration Data and Performance	14
	Calibration	14
	Noise, Stability and Interference	14
5	Installation and Set-up	18
6	Operation and Maintenance	21
	Controls: Location and Functions	21
	Normal Operation	24
	Maintenance and Troubleshooting	25
7	Electrical Circuits	27
8	Electronic Circuits of Optics Assembly	30
	Main Electronics Card	30
	Reference Card	33
	Preamplifier	33
	Range Card	33
9	Digital Processor Assembly	41

SECTION 1

INTRODUCTION AND SUMMARY

The monitor described herein has been designed for use with a device to measure the concentration of non-methane hydrocarbons (NMHC) in ambient air. In the first step of the process, the CO_2 is scrubbed from the air to be sampled; this process also removes most of the H_2O vapor. The next step involves a catalyst that causes the oxidation of the NMHC to form H_2O and CO_2. The CO_2 channel of the CO_2-CO monitor measures the concentration of the CO_2 produced, which is directly related to the concentration of NMHC. Carbon monoxide in the air is also oxidized to form CO_2; therefore, it is necessary to account for the amount of CO_2 produced by the oxidation of CO if the NMHC concentration is to be determined accurately. This is accomplished by using the CO channel of the monitor to measure the concentration of CO in the air before it passes through the oxidation stage. The difference between the measured concentrations of CO_2 and CO is the concentration of carbon atoms in the NMHC.

Two requirements for the CO_2-CO monitor played an important role in the design: (1) the minimum detectable concentration of each gas must be less than about 0.02 ppm, and (2) the volumes of the sampling sections must be kept small. The second requirement results from the need to maintain a short sample "turnover" time without using an excessive amount of gas. The rate at which the NMHC can be oxidized to form CO_2 is a limiting factor; therefore, it is important that the CO_2 sample cell be small. Multiple-pass optics operated at 22 passes in the sample cells make it possible to achieve the required sensitivity in the relatively short sample cells. The approximate base lengths and volumes of the sample cells are, respectively: CO_2, 30 cm and 315 cm^3; CO, 40 cm and 640 cm^3.

The analysis section of the monitor consists of two basic assemblies, the optical assembly and the digital signal processor. The electrical outputs from the optical assembly are two analog signals; one signal is related non-linearly to the CO_2 concentration, the other to the CO concentration. These analog signals serve as inputs to the digital signal processor, the first stage of which is an analog-to-digital converter. The resulting digital signal for each channel is processed to account for the non-linearity in the relationships between gas concentrations and the output analog signals of the optics assembly. Three digital meters on the optics assembly give continuous readouts of: (a) CO_2 concentration, (b) CO concentration, and (c) the difference ((a) - (b)). The third reading is equal to the concentration of NMHC in the air being sampled.

Also included with the digital assembly are three analog output jacks with the signal on each jack directly proportional to the corresponding digital readout. Thus, these analog voltages are directly proportional to the gas concentrations because the non-linearities in the relationships between concentrations and output signals of the optics assembly have been accounted for in the processor.

The zero-setting of the monitor is quite stable although it should be checked 2 or 3 times per hour if the best possible accuracy is required. When using 10-second electronic time constants, the peak-to-peak noise

equivalent concentrations are approximately 0.015 ppm of CO_2 and 0.04 ppm of CO. The minimum detectable concentrations are approximately one half the peak-to-peak noise-equivalent concentrations if the signal is observed for as long as 20-30 seconds.

SECTION 2

LAYOUT OF OPTICAL ASSEMBLY

GFC AND ENTRANCE OPTICS

The optical assembly contains two similar but separate channels, one for CO and one for CO_2. Figure 1 shows a perspective view of the entrance optics for both channels. Infrared energy from a hot source passes through window WC1 into the prism PC1; at the beveled surface of PC1, the beam is reflected through 90^o to lens LC1 and into prism PC2. A beveled surface at the opposite end of prism PC2 reflects the beam out of the side of the prism and through the rotating gas-filter cell (GFC) to filter C and lens LC2. From there, the beam continues through prism PC3 to the CO sample cell discussed in the following sub-section. The reflecting surfaces of CaF_2 prisms PC1, PC2, and PC3 are aluminized. Lenses LC1 and LC2 are also made of CaF_2; lens LC1 images the source near filter C, which passes a narrow spectral band centered near 4.6 micrometers where CO absorbs strongly. Field lens LC2 forms an image of lens LC1 near the entrance window of the CO sample cell. Sapphire window WC1 is anti-reflection coated for wavelengths near 4.6 micrometers and protects the brittle CaF_2 prism PC1 from heat shock due to the hot source.

Prisms PD1, PD2, etc., of the upper optical path are part of the CO_2 channel. This optical path is similar to the corresponding one for the CO channel except that filter D passes a narrow spectral interval near 4.3 micrometers where CO_2 absorbs strongly.

The prisms with reflecting surfaces are used instead of flat mirrors to reduce to optical path through air, and thus to reduce errors due to absorption by CO and/or CO_2 in the air. Variations in the amount of this absorption cause changes in the zero-settings. All of the components illustrated in Figure 1 are enclosed in a sealed aluminum box called the GFC enclosure. A teflon O-ring seal fits around the motor shaft. The box is flushed with dry air that is free of CO and CO_2 to reduce further any error due to either of these gases in the optical path. The end of prism PD3 is within one mm of the entrance window of the CO_2 cell; prism PC3 is a similar distance from the CO cell. These air gaps are within the enclosure and are flushed. The total optical path through the air in the enclosure is less than one cm in each of the channels. Keeping air out of the optical path is more important for the CO_2 channel than for CO because normal air contains more than one hundred times as much CO_2 as CO.

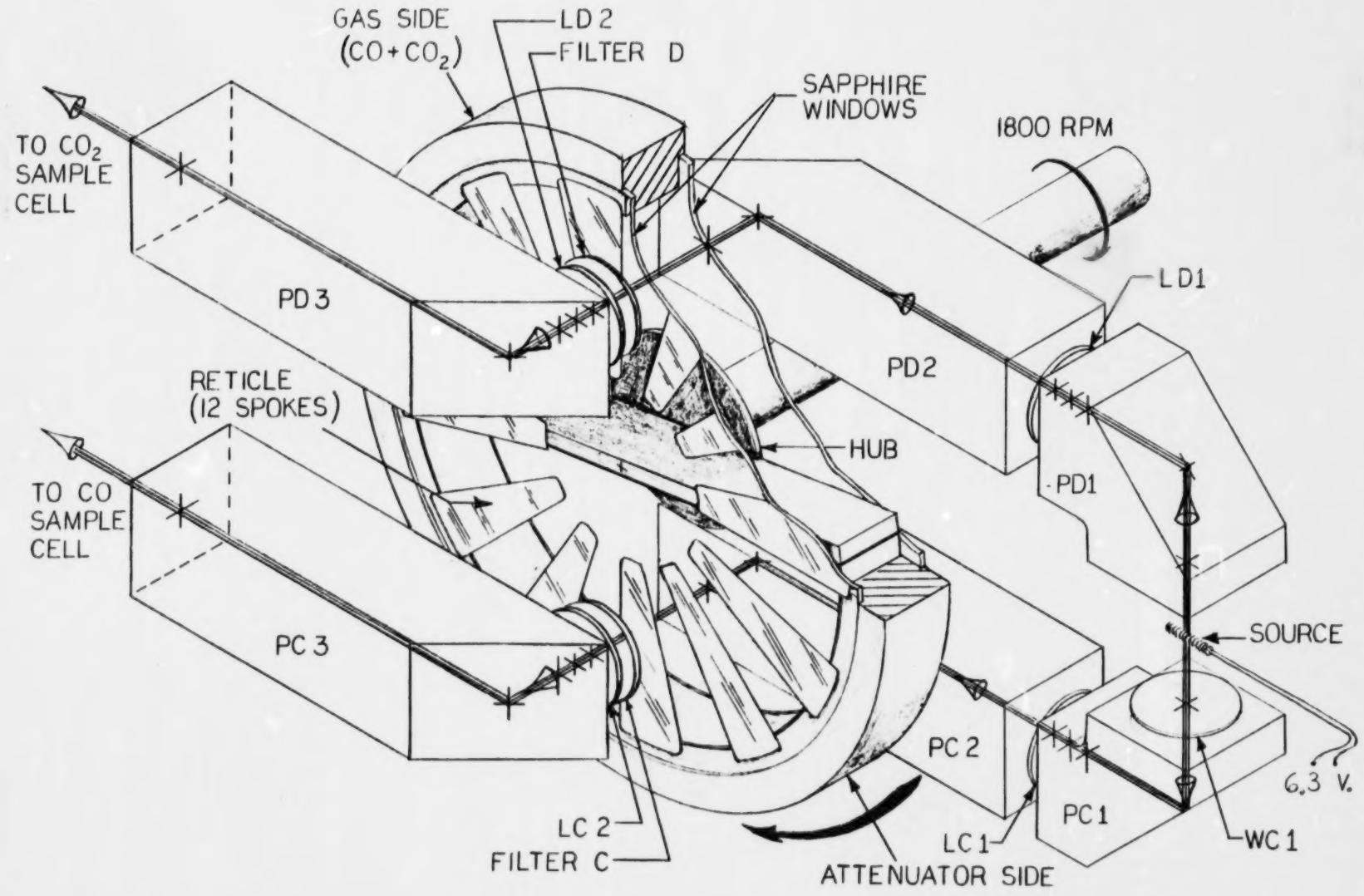

Figure 1. Optical diagram of the source optics. Infrared energy from an electrically heated source follows two different paths, one to each of the sample cells. All of the components shown are within an enclosure that is flushed with N_2 or argon to reduce absorption by CO_2 in the air. The gas-filter cell (GFC) rotates at 1800 rpm.

The sapphire windows of the GFC are 6.35 cm (2.5 inches) in diameter and are spaced 0.6 cm apart. One-half of the GFC is filled with a mixture of CO and CO_2; the other half contains a semi-circular piece of CaF_2 that fills the space between the windows. The hub is bonded concentrically to one window of the GFC. As the GFC rotates at 30 rps, each radiant energy beam passes alternately through the CO_2-CO mixture and the CaF_2. Twelve opaque reticles chop the beams at 360 Hz. The operating principles and more details of the GFC are given in Section 3.

SAMPLE CELLS AND DETECTORS

Figure 2 shows a top view of the optics in the multiple-pass cell that contains the CO_2 sample. Radiant energy from prism PD3 enters the sample cell through lens LD3, which serves as the entrance window and forms an image of the source near spherical mirror S2. This mirror forms an image of LD3 on spherical mirror S3, the first mirror of the multiple-pass optical system. After passing the length of the cell 22 times, the radiant energy is directed by flat mirror S6 through the exit lens LD4, which also serves as the exit window and images mirror S3 on the 2 mm x 2 mm PbSe element of the detector. The distance from mirror S4 to either S3 or S5 is 30 cm, making the total optical path length in the cell approximately 665 cm.

The CO cell is similar to the CO_2 cell and is mounted directly beneath it. Mirrors S1, S2 and S6 are mounted identically in both cells, but the CO cell is longer and wider. The distance from mirror S4 to either S3 or S5 is 40 cm in the CO cell and 30 cm in the CO_2 cell. Thus, the optical path length in the CO cell, which is also adjusted to 22 passes, is approximately 885 cm. The internal width of the CO_2 cell is 4.8 cm, whereas the same dimension of the CO cell is 7.3 cm. The internal height of both cells is 2.2 cm.

Figure 3 shows the image patterns on mirrors S4 of both cells. The numbers adjacent to the images in the lower cell represent the number of passes made by the beam when the image is formed. Images 2, 6, 10, etc., are formed by mirror S3, and images 4, 8, 12, etc., are formed by mirror S5. Note that each radiant energy beam enters the upper portion of the cell and exits from the lower portion.

Each sample cell and its associated gas lines are designed so that each samples gas from a different source. The gas flows into one end of the cell and out the opposite end. The end flange contains several small holes (not shown in Figure 2) through which the gas enters the cell. Passing the gas through these holes reduces "jet streams" that would mix the incoming gas with the gas already in the cell. Thus, the gas travels in nearly a "plug flow," which is desirable to reduce the amount of gas required to completely flush out one sample and replace it with a new one.

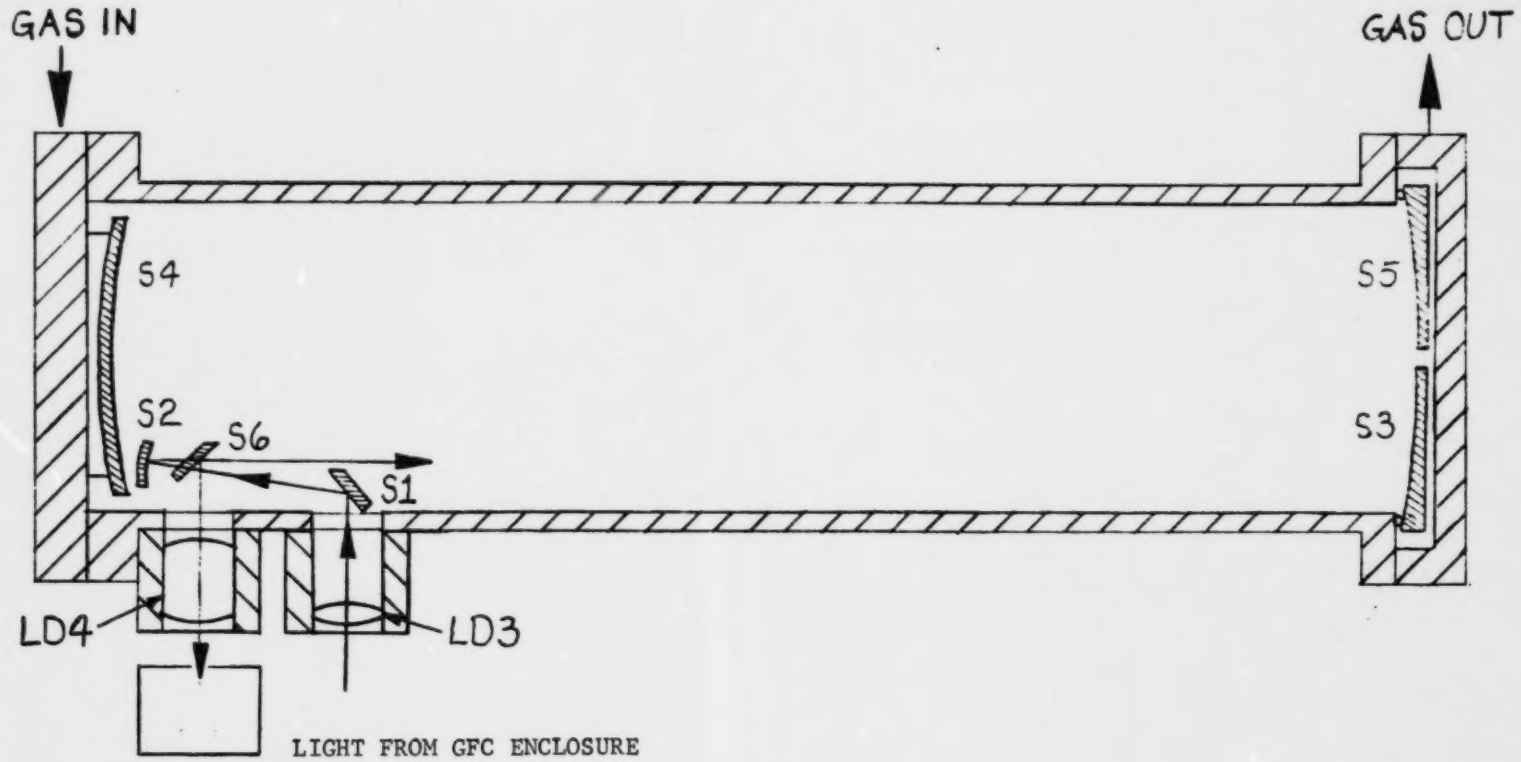

Figure 2. Top view of the optics in the multiple pass CO_2 cell. The CO cell is schematically the same but dimensionally longer and wider.

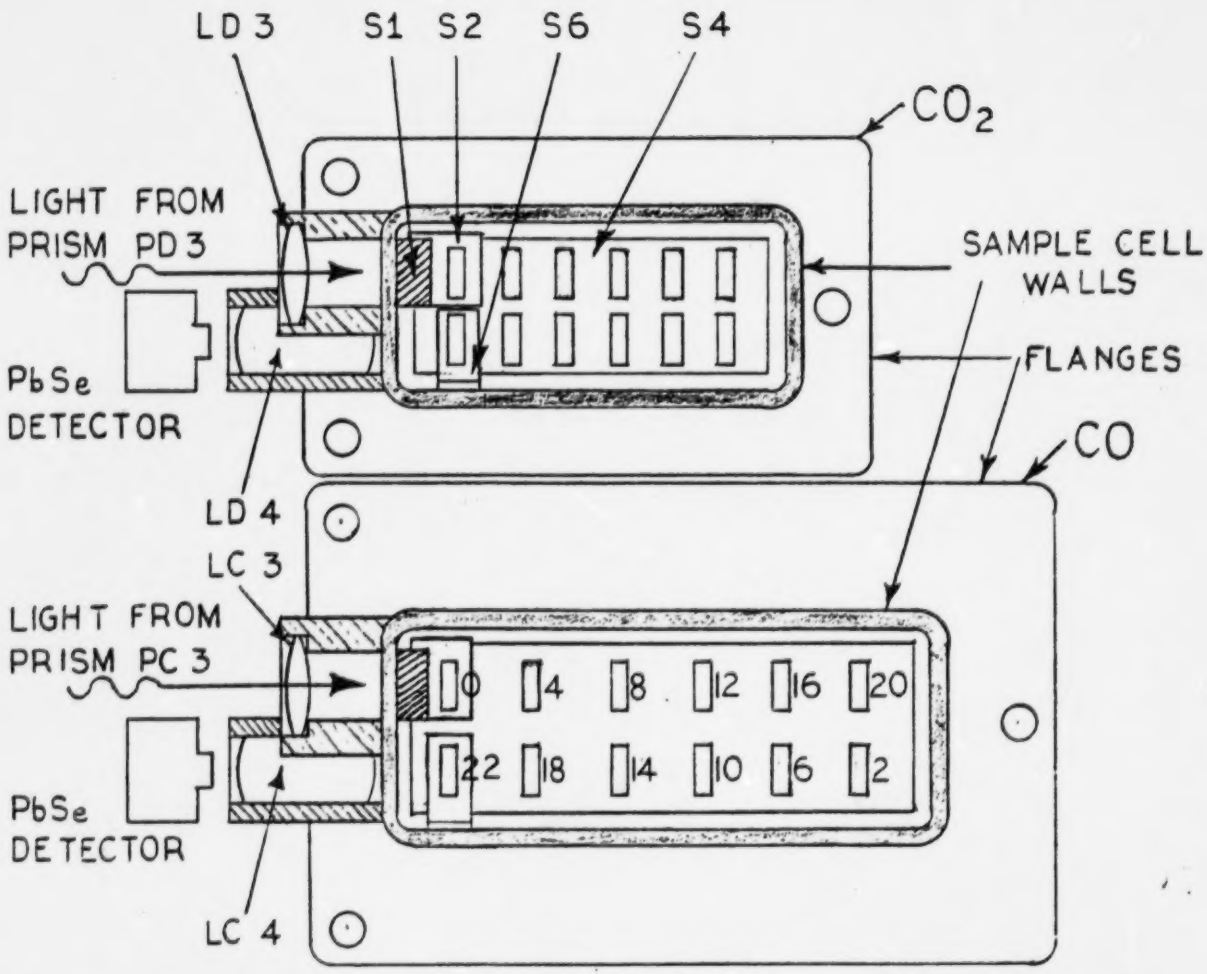

Figure 3. Image patterns on mirrors S4 of the CO_2 and CO sample cells. The relative positions of the two sample cells and detectors are as indicated.

Two important factors were considered in making the CO_2 cell smaller than the CO cell: (1) less CO_2 than CO is available from the scrubber/catalytic oxidizer to be used with the analyzer; (2) a longer optical path is required for CO than for CO_2 to obtain the desired sensitivity because the CO_2 absorption lines are much stronger than the CO lines. The concentrations of both CO and CO_2 can be monitored either while the gases flow continuously through the cells or when the gas flow is stopped. Zero-settings for both channels are adjusted with zero-gas flushing through the sample cells. High-purity N_2 is normally adequate as a zero-gas for CO_2, but the N_2 frequently contains a few hundred ppb of CO and can, therefore, not be used reliably as a zero-gas for the CO channel. High-purity argon is usually free of a significant amount of either CO or CO_2.

Both sample cells are wrapped with heating wire and are temperature controlled at approximately 45°C. Nearly uniform temperature is maintained by applying extra heat to the end plates and flanges with electrical resistors imbedded in them. The cell bodies are made of stainless steel because of its low coefficient of thermal expansion and resistance to chemical reactions and adsorption of gas on the surface. Maintaining the cell above normal ambient temperature reduces the amount of adsorption and makes it convenient to control the temperature with a simple controller and heating circuit.

The lower cell (CO) is mounted to the baseplate on a three-point suspension. A shank with a precision ball ground on one end is pressed into the baseplate, and the ball fits into a cone-shaped socket in the bottom side of the end flange on the end near the detector. Another ball mount fits into a V-groove on the bottom side of the cell near the end containing mirrors S3 and S5. A third ball rests against a flat surface on the bottom side of the same end flange that has the cone socket, but on the side away from the detector. The cell is spring-loaded down against the three ball supports, allowing the cell to expand or contract from the ball in the socket. This avoids misalignment of the optics due to distortion of the cell that might occur if the cell were mounted rigidly to the aluminum baseplate. The upper cell (CO_2) is mounted to the lower cell by a similar three-point suspension.

A small sleeve, not shown in Figure 2, encloses the air space between the detector and the exit window of the CO_2 sample cell. A seal is formed by flexible silicone cement that bonds the sleeve to the detector mount and the exit port of the sample cell. The enclosed volume is flushed with dry air from the same line that flushes the GFC enclosure. A similar sleeve connects the CO sample cell to the corresponding detector. Because of less need to reduce the atmospheric path in the CO channel, the space between the exit window and the detector is not flushed. The enclosure adequately reduces variations in the amount of CO in this short optical path.

The 2 mm x 2 mm element of each PbSe detector is cooled thermoelectrically to approximately -25°C to increase the sensitivity. The sensitive element is slightly larger than the image formed on it.

SECTION 3

PRINCIPLES OF OPERATION OF OPTICAL ASSEMBLY

The principles of detection of the monitor are based on the well-proven gas-filter correlation techniques that have been developed at Aeronutronic and several other laboratories. Two articles[1,2] published by Aeronutronic scientists discuss in great detail, but in simple terms, the basic principles of gas-filter correlation monitors. The following two sub-sections summarize these principles as they apply to the CO_2-CO monitor.

GFC AND PRINCIPLES OF DETECTION

Much of the good stability and high sensitivity of the instrument is due to the rotating GFC illustrated in Figure 1. The GFC consists of 2 semi-circular compartments divided along a diameter. The gas side is filled to 550 torr with a mixture of 97.2% CO and 2.8% CO_2. The attenuator side has a semi-circular piece of CaF_2 filling the gap between the sapphire windows so that there is no CO or CO_2 in the beam when it is passing through the attenuator side. The sapphire windows have anti-reflection coatings on the surfaces in the gas side. Reflection from the CaF_2 and sapphire surfaces in the attenuator side attenuate the beam so that the average transmittance is approximately the same as the transmittance through the gas side.

A reticle deposited on the surface of one of the GFC windows has 12 opaque strips and 12 openings to produce a high-frequency chopping rate of 360 Hz. When CO is added to the sample section, it absorbs a fraction of the chopped energy that passes through the attenuator side of the rotating GFC. However, when the gas side of the GFC is in the beam, the GFC absorbs most of the energy at wavelengths where the CO in the sample cell absorbs. Therefore, the addition of CO in the sample cell decreases the energy passing through the attenuator more than it reduces the energy through the gas side of the GFC. Thus, the 360-Hz chopped signal contains a modulation at 30 Hz, the rotational frequency of the GFC. The amount of modulation depends on the product of the CO concentration and optical path length in the sample cell. The detector signal is processed by the electronics to produce a dc output signal proportional to the fractional modulation of the energy incident on the detector, and thus to the concentration of CO in the sample cell.

---

1. Burch, D.E. and Gryvnak, D.A., "Cross-Stack Measurement of Pollutant Concentrations Using Gas-Cell Correlation Spectroscopy". Chapter 10 of Analytical Methods Applied to Air Pollution Measurements, Stevens, R.K. and Herget, W.F., (eds), Ann Arbor Science Publishers Inc., 1974.

2. Pembrook, J.D. and Burch, D.E., "A Multigas Analyzer for Automobile Exhausts", Proc. of SPIE, Vol. 95, 84-91 (1976).

Any absorbing gas species other than CO in the sample cell will not produce a 30-Hz modulation if there is no correlation between the spectral structures of the gas and the CO in the GFC. When there is no correlation between the spectral structures, the gas absorbs exactly the same fraction of the energy passing through the GFC as that passing through the attenuator. Thus, under this idealized condition, no 30-Hz modulation is produced and there is no interference in the output signal by the gas. Of course, the instrument cannot operate properly if the absorbing gas absorbs a large fraction of the radiant energy incident on it. Unfortunately, there is usually a small amount of correlation between the spectral structures of the gas species to be detected and another gas that absorbs in the same spectral region. There is a slight positive correlation between the spectral structures of CO and H_2O in the spectral bandpass of the CO channel. Thus, H_2O in the sample produces a small positive interference signal. This slight interference is negligible when the monitor is used for its intended purpose because most of the H_2O vapor is removed by the sample conditioner from the air being sampled.

ELECTRONICS AND PROCESSING OF DETECTOR SIGNALS

The signal-processing electronics contain two nearly identical channels, one for CO and one for CO_2. A block diagram of the electronics for the CO channel is shown in Figure 4. A single panel meter and single reference pick-up with its associated tuned reference amplifier serve for both channels. The empirical relationship between the output signal and the CO (or CO_2) concentration has been determined experimentally by calibrating the instrument with samples of known CO (or CO_2) concentrations. The calibration data have been used to program the digital assembly so that non-linearity in the relationship between CO concentration and output signal is accounted for and the digital readout is in ppm concentration.

The 360-Hz component of the signal from the detector serves as the carrier for the 30-Hz component that is to be measured. The 30-Hz component of the detector signal resulting from any 30-Hz variation of radiant energy on the detector that is not also chopped at the carrier frequency is rejected by the electronics. The electronics consist basically of two demodulators in series. The first demodulator operates at the carrier frequency, 360 Hz; the average output of this demodulator is proportional to the amount of radiant energy chopped at 360 Hz. If the chopped energy incident on the detector is also modulated at 30 Hz, the 30-Hz component of the output signal from the 360-Hz demodulator is proportional to the modulation. This 30-Hz component then passes through a series of gain controls and amplifiers to the 30-Hz synchronous demodulator. The output of the 30-Hz synchronous demodulator is proportional to the 30-Hz modulation of the 360-Hz signal, and thus to the concentration of CO in the sample gas. The reference signal for the 30-Hz synchronous demodulator is supplied by the 30-Hz reference pick-up.

During the normal mode of operation, it is desirable that the output signal be proportional to the ratio, $V_a/V_c = V'$, where V_a is the average

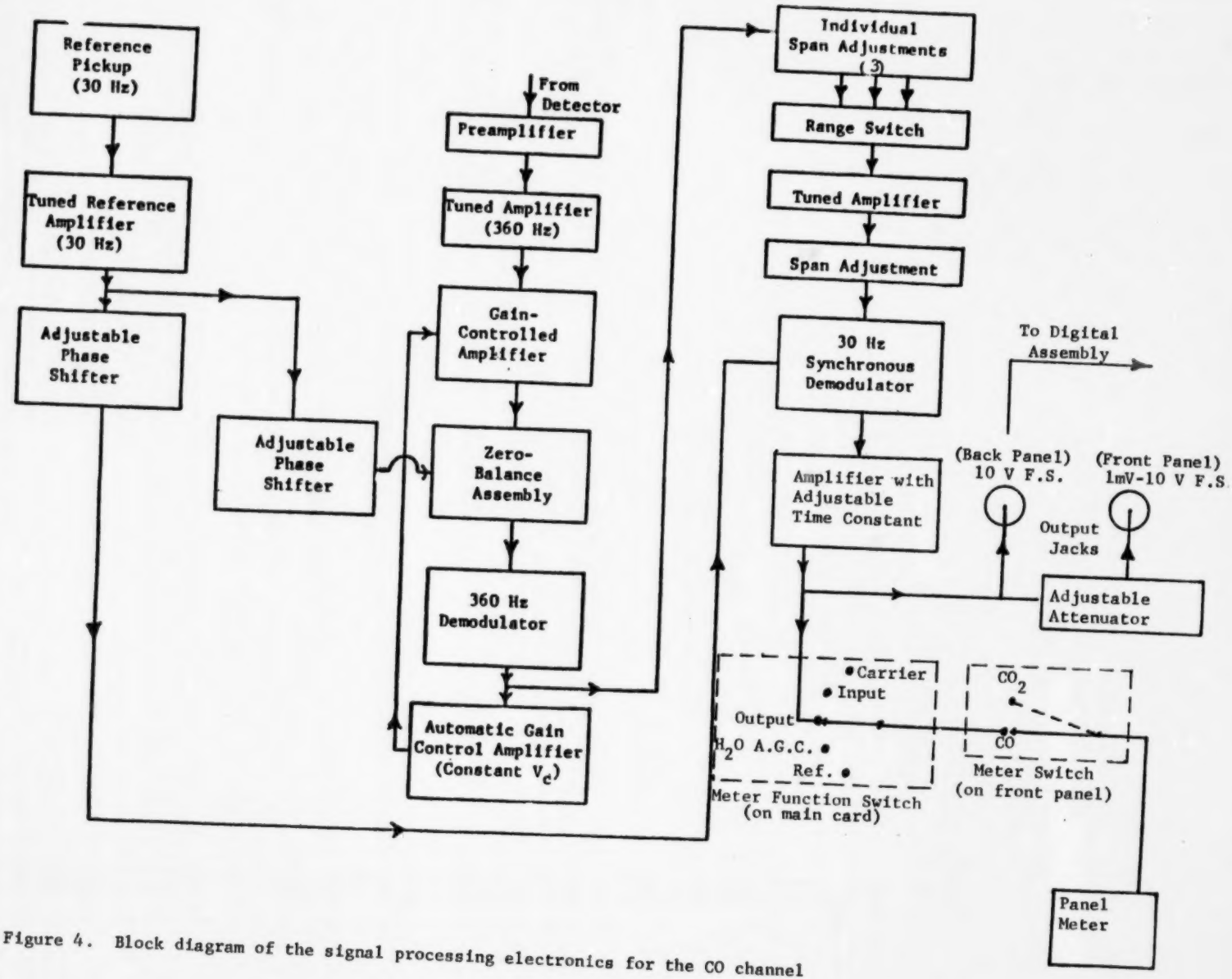

Figure 4. Block diagram of the signal processing electronics for the CO channel

demodulated 30-Hz component of the detector signal and V_c is the 360-Hz component of the detector signal. The instrument calibration relates the CO concentration of the sample gas to V', and it is desired that this relationship be independent of source brightness, detector sensitivity, etc. During the normal mode of operation, V_c is maintained at a constant value by the automatic gain control (AGC) circuits. If, for example, the signal from the detector decreases because of dirt on a window or a decrease in source brightness, the AGC increases the amplification of both the 360-Hz signal and the 30-Hz signal by the same factor. Therefore, V' is kept directly proportional to the output V_a and maintains a constant relationship with the CO concentration.

A time-constant switch mounted on the main electronics card makes it possible to select an electronic time constant of 0.3, 1, 3 or 10 sec. The main output signal can be determined from the panel meter or from either of two output jacks. A signal that corresponds to a full-scale reading of the panel meter produces a 10-volt dc signal on the main output jack, which is connected by an external cable to the input jack of the digital assembly. The corresponding full-scale reading for the other output jack, which is mounted on the front panel of the optics assembly, can be adjusted from less than 1 mv to 10v. This adjustment is made with a switch and potentiometer on the main electronics card. Thus, the instrument can be used with a wide range of recorders or meters, provided the input impedance of the recorder is sufficiently high.

A four-position selector switch mounted on the main electronics card makes it possible to use the panel meter to monitor quantities other than the output signal. The 30-Hz reference signal and the average carrier voltage, V_c, can be checked to see if the signals are in the correct operating range. When the selector switch is in the "signal-in" position, the signal displayed on the meter is equal to the signal going into the 360-Hz demodulator. With the selector switch in the "signal out" position, the meter reading is proportional to the output signal. The signals on the output jacks are not affected by the position of the selector switch. When the switch is in the "H_2O AGC" position, zero voltage is across the panel meter, making it convenient to adjust the zero position of the meter. This switch position was originally designed for use with circuits not employed in this instrument.

The 30-Hz reference pickup, which consists of a light-emitting diode (LED) and a small phototransistor, is mounted near the motor on the end opposite the GFC. As a semi-circular blade mounted to the motor shaft spins at 1800 rpm, the light reflected from the blade is sensed by the detector and produces a 30-Hz signal. The amplifier for the 30-Hz reference pickup is tuned and contains an adjustable phase shifter to produce a "clean" signal with the proper phase for the 30-Hz synchronous demodulator.

The zero-balance assembly electronically accounts for any misbalance between the two halves of the GFC cycle when there is no CO in the sample cell. This electronics assembly would not be required if it were practical

to maintain a perfect optical balance between the two filters on the filter wheel. Approximately ± 10 percent variation in the transmittance through the GFC during either of the two halves of the cycle can be accounted for by this electronic zero-balance assembly. The assembly decreases the amplification ahead of the 360-Hz demodulator during one of the halves of the GFC cycle. The proper half of the cycle during which the amplification is changed is selected by a switch on the front panel. A signal from the 30-Hz reference pickup switches the zero-balance assembly between the two different gains with the proper phase. The difference in the gains between the two halves is adjusted with the "zero" potentiometer mounted on the front panel of the instrument. The CO channel contains two zero potentiometers, one for coarse and one for fine adjustments, whereas the CO_2 channel, which does not require fine adjustment, contains only one potentiometer.

SECTION 4

CALIBRATION DATA AND PERFORMANCE

CALIBRATION

Figures 5 and 6 show the calibration curves for CO_2 and CO, respectively. Each figure contains three curves, one for each of the three ranges of sensitivity, 1 ppm, 5 ppm, and 20 ppm full-scale. A single range switch on the front panel of the optics assembly changes the sensitivity ranges of the two channels simultaneously so that both are always on the same range. Voltages plotted in Figures 5 and 6 correspond to the signals at the main output packs on the rear panel of the optics assembly. Full-scale readings correspond to 10 volts. The output signals can also be determined from the panel meter if the meter-function switches on the main electronics cards are turned to the positions labeled "output". The voltage on an output jack on the front panel varies from the corresponding one on the rear panel by a constant factor determined by the settings of a switch and potentiometer on the main electronics card.

Portions of the curves corresponding to very low concentrations on the log-log scales have unity slopes, which correspond to linear relationships between the gas concentration and the corresponding analog output voltage of the optics assembly. The linear relationship applies to CO for concentrations less than approximately 4 ppm; however, this simple relationship holds only for CO_2 concentrations less than approximately 0.4 ppm.

Seventh-order polynominals were fitted to the curves in Figures 5 and 6. These equations were then programmed into the digital assembly so that gas concentrations are calculated from the analog voltages.

NOISE, STABILITY AND INTERFERENCE

The CO_2 absorption lines in the spectral band used to detect this gas are much stronger than the corresponding lines of CO. Therefore, higher electronic gain is required in the CO channel than in the CO_2 channel to produce the same voltages for a given concentration. This higher electronic gain produces a correspondingly higher noise-equivalent concentration in the CO channel. Most of the noise on the output signal of the CO channel is apparently due to detector noise and is equivalent to approximately 0.04 ppm (peak to peak) when a 10-second electronic time constant is used. The corresponding noise level for the CO_2 channel is only about 0.015 ppm.

The responsivity of either channel of the monitor is quite stable, and variations in this quantity are normally too low to cause significant

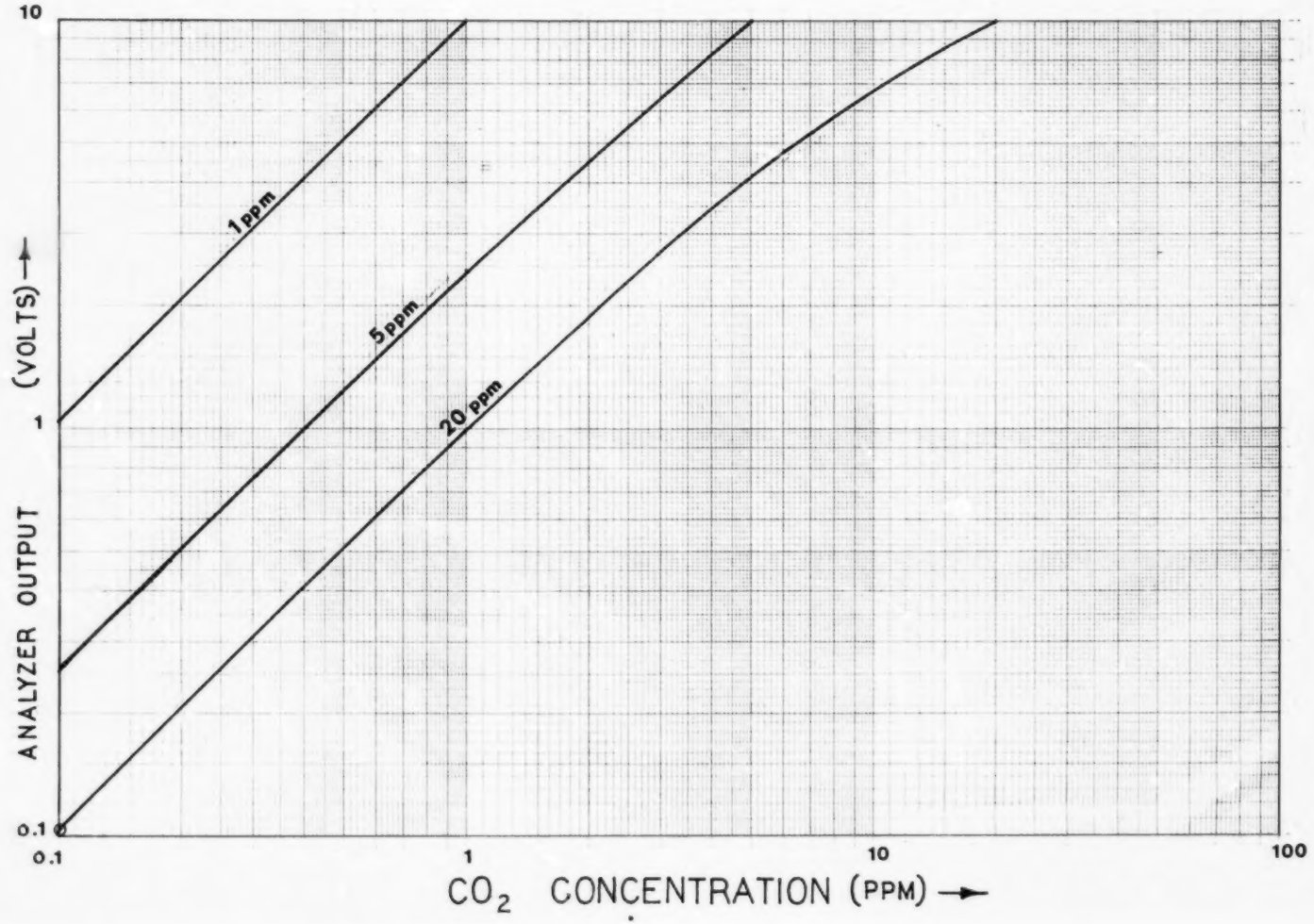

Figure 5. Calibration curves for the CO_2 channel of the CO_2-CO monitor.

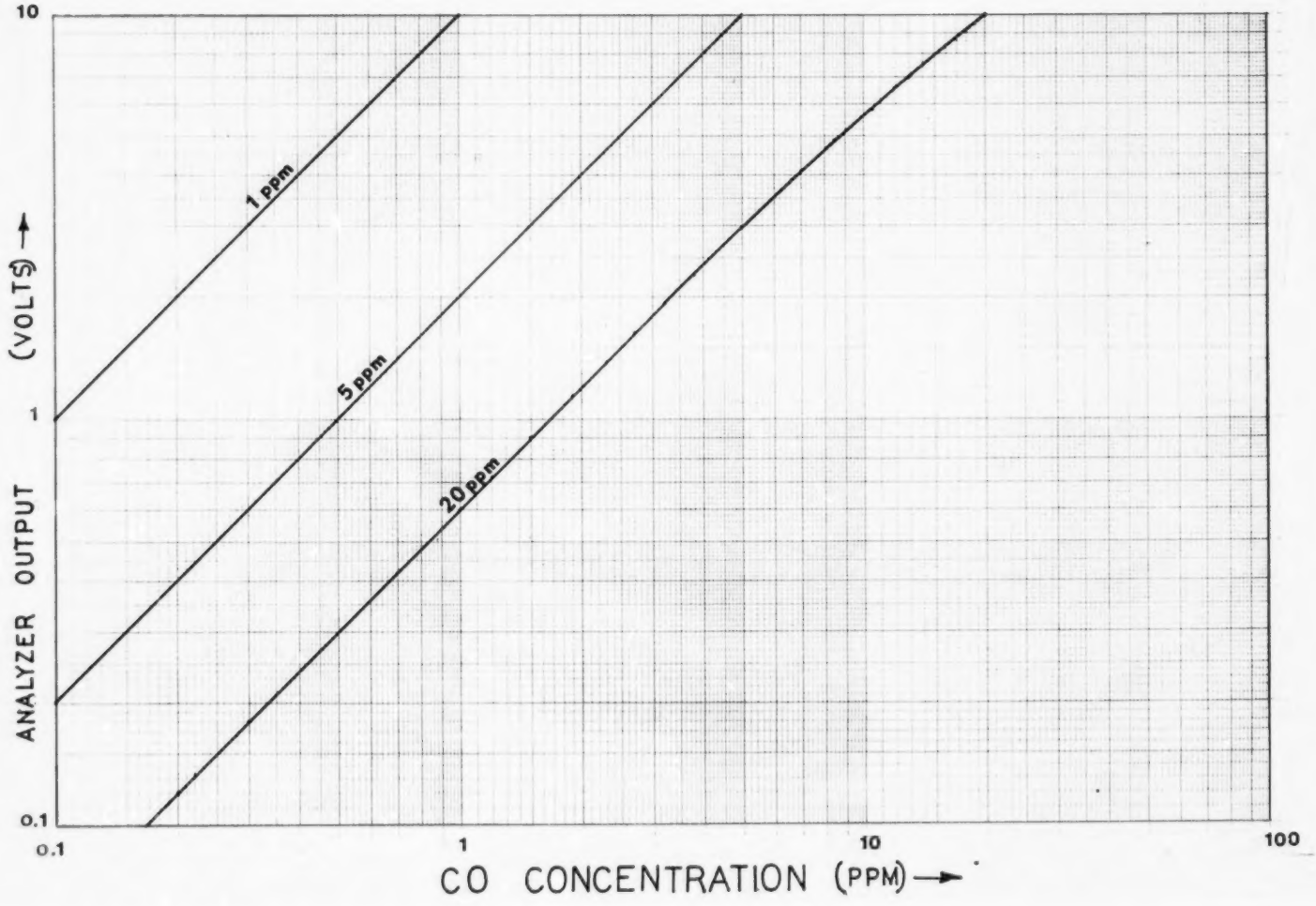

Figure 6. Calibration curves for the CO channel of the CO_2-CO monitor.

errors in the measurements. Variations in the zero-setting (corresponding to no absorbing gas in the sample cells) may produce significant errors, particularly if the monitor has not been turned on long enough to stabilize. Changes in temperature are the main causes of variations in the zero-settings; such variations are maintained at a relatively low-level during normal operation by controlling the temperatures of the sample cells and the GFC enclosure. Serious drifts in the CO_2 channel can result if the GFC enclosure is not flushed adequately (typically greater than 0.5 liter per minute.)

No significant error is expected due to interference by any normal atmospheric gases, except possibly H_2O. An H_2O concentration of 0.2% (2000 ppm H_2O)produces erroneous readings of approximately +0.1 ppm of CO. For H_2O concentrations below 0.5%, it is appropriate to assume that the error signal is proportional to the H_2O concentration. Under normal operating conditions, the H_2O concentration is expected to be low enough that the interference is negligible. Interference by other atmospheric gases is insignificant as long as most of the H_2O vapor is removed by the CO_2 scrubber.

SECTION 5

INSTALLATION AND SET-UP

The two assemblies are separate and can be used on a bench top, or they can be mounted in a standard 19" instrument rack. After the two assemblies are put in place, the three jacks on the back panel of the optics assembly are connected by three cables to the three corresponding jacks on the back panel of digital assembly. A fan forces cooling air through the inside of the optics assembly, but the rack must be open enough that the air surrounding both assemblies is free to circulate.

The digital assembly can be mounted in a standard 19" rack from the front in the normal manner. However, the optics assembly is too wide to be mounted from the front; it must be put into position, either directly above or directly below the digital assembly, from the rear of the rack by following procedure (see Figure 7).

1. Bolt the "dog-leg" brackets loosely to the front of the rack chassis with the tabs protruding inward at the bottom. Be sure that the ¼" holes at the top clear the face of the rack chassis.

2. Two people lift the monitor in from the rear until the slots in each side of the bottom surface of the baseplate mate with the protruding tabs in the dog-leg brackets. Let the front of the monitor rest on these two protruding tabs.

3. Lift the rear of the monitor to a level position so that the uppermost holes in the dog-leg mounting brackets align with the holes in each side of the monitor.

4. Insert ¼" x 20 bolts (1½" minimum length) through the holes in the dog-leg brackets and into the sides of the monitor.

5. Tighten the bolts that hold the dog-leg brackets to the rack chassis.

6. Use one of the two standard BNC cables supplied with the monitor to connect the CO_2 output jack on the back of the optics assembly to the CO_2 input jack on the back of the digital assembly. Use the other BNC cable to connect the corresponding CO jacks that are adjacent to the CO_2 jacks.

7. Use the range cable to connect the range-select jack on the rear panel to the corresponding jack on the digital assembly.

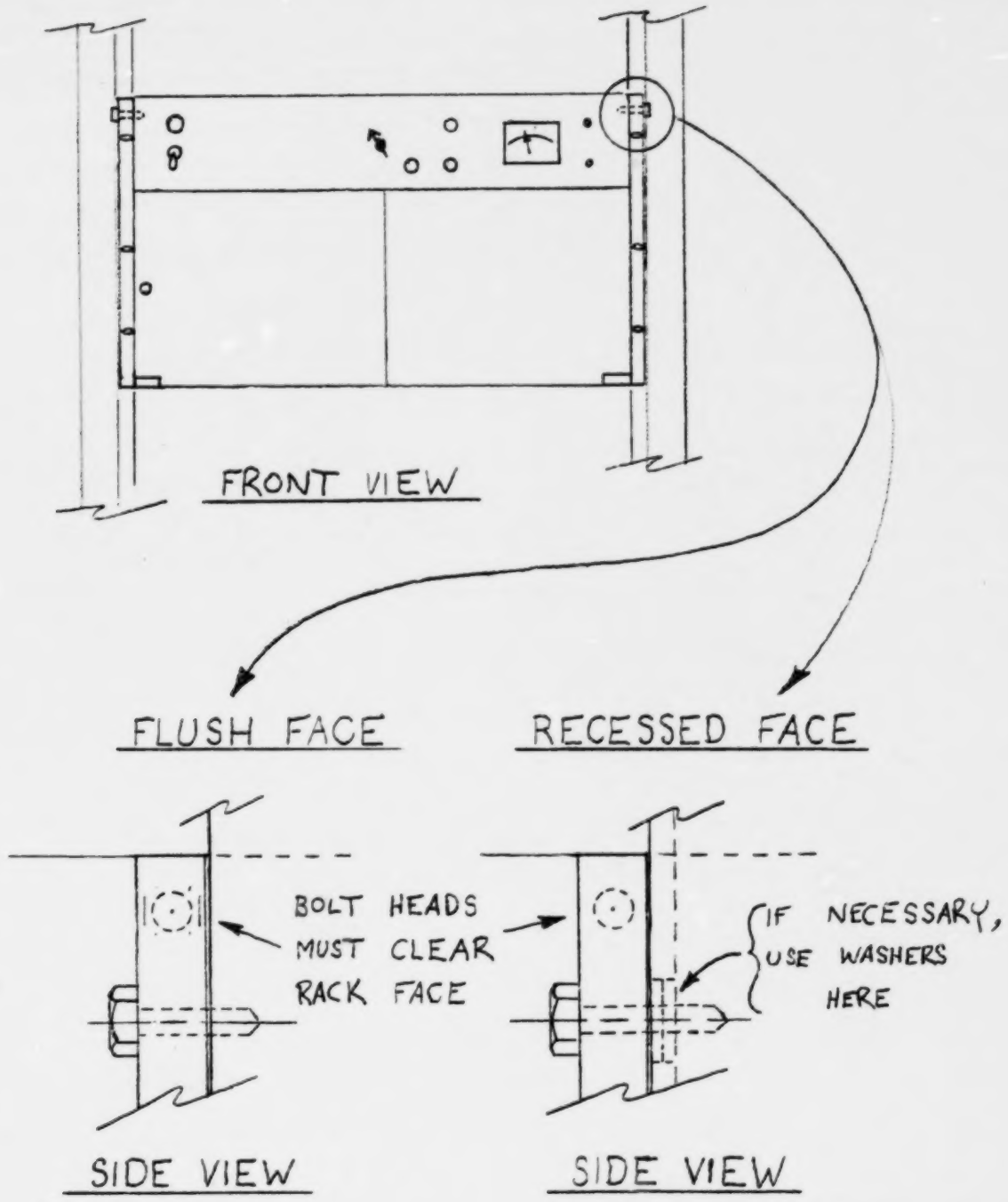

Figure 7. Mounting brackets for the optics assembly.

52<

8. Analog recorders or voltmeters may be connected either to the output jacks on the digital assembly or to the output jacks on the front of the optics assembly. The analog voltages on the output jacks of the digital assembly are directly proportional to the respective concentrations. The analog voltages on the jacks on the front panel of the optics assembly are related non-linearly to the concentrations. (See Section 6 for the method of relating the voltages to the concentrations.)

9. Insert the power plugs of both assemblies into a standard 60-Hz power line with AC voltage between 105 and 120 V. Both units should be plugged into a common line.

10. Connect the appropriate gas sample lines to the four Swagelock connectors on the rear of the optics assembly. There are two inlet lines and two outlet lines, one of each for CO_2 and CO.

11. Connect another line to the connector used to flush the GFC enclosure. This line is to be connected to a supply of gas that is free of CO_2 and CO. A flow rate of 3-10 liters per minute is recommended for the first few minutes; after the enclosure is adequately flushed, a flow rate of 0.5-1 liter per minute is usually adequate.

SECTION 6

OPERATION AND MAINTENANCE

The instructions given in this section are to be followed after the monitor has been installed and the zero-gas lines and sample gas lines have been connected. Best stability is attained if the monitor has been turned on for more than approximately two hours and the GFC enclosure has been flushed with zero gas. It is recommended that the monitor be left turned on overnight if it is to be used the next morning.

CONTROLS: LOCATIONS AND FUNCTIONS

Power Switch

The main power switch in the upper, left-hand corner of the front panel connects or disconnects 115V, 60-Hz power to the entire optics assembly.

Panel Meter, Channel Switch and Meter Function Switch

The panel meter and its associated channel switch are located on the front panel; the position of the channel switch (denoted "meter") determines which channel (CO_2 or CO) is connected to the meter. The same procedures are followed for each channel.

The signal displayed by the panel meter depends on the position of the meter function switch located on the lower, left-hand corner of the main electronics card (see Figure 11). Four different signals can be displayed: reference, output (proportional to concentration of CO or CO_2 in sample gas), input, or carrier. In the following discussions, meter readings are given in meter units, where 100 meter units correspond to full scale. When the meter function switch is in the output position, 100 meter units corresponds to a full-scale reading of 10 volts on the main output jack on the back panel of the instrument.

Zero Adjustments

The 10-turn potentiometers used to adjust the zero settings are located on the front panel. A single potentiometer serves the CO_2 channel, but two are used for the CO channel, one for coarse and one for fine adjustments. When the switch adjacent to a potentiometer is in the "+" position, increasing the dial reading of the potentiometer changes the output signal in the direction corresponding to more CO or CO_2. Changing the switch to the "-" position reverses the effect of the potentiometer. When the switch is in the center (off) position, the output signal remains the same as if the potentiometer were adjusted to give a zero reading on its dial.

Before obtaining data on CO or CO_2 concentrations, the sample cells and the enclosure should be flushed with zero gas and the zero potentiometers adjusted to produce zero output signal. The zero-setting should be checked periodically while data are being obtained to account for gradual changes. The stability of this setting depends mostly on the stability of the instrument temperature; the rate of flushing of the GFC enclosure may also have an effect on the zero-setting of the CO channel.

At the time the monitor was delivered to Aerochem, the dial readings on the zero potentiometers corresponding to zero output signal were: CO_2 channel + 5.85; CO channel, coarse + 2.60, fine + 5.00. It is recommended that the operator maintain a record of the potentiometer settings because such a record may be helpful in diagnosing problems.

Signal Readouts

An output signal that is directly related to the concentration of either CO_2 or CO can be measured or readout at 5 different places: (1) panel meter, (2) front-panel jacks, (3) rear-panel jacks (normally connected to the digital assembly), (4) digital readout on digital assembly and (5) analog output jacks on digital assembly.

The signal from either channel (CO_2 or CO) may be displayed on the analog panel meter on the optics assembly; the choice of channel depends on the position of the meter switch adjacent to the meter. In order to determine the output signal from the panel meter, the meter function switch on the main electronics card must be in the "output" position.

The signal on the front panel jack due to a given gas concentration depends on the settings of the recorder potentiometer (labeled R69 REC) and the switch (REC SW) on the main electronic card (see Figure 11). Full-scale readings can be adjusted from less than 1 mV to 10V. The relationship between the voltage and the gas concentration is given by the appropriate calibration curve in either Figure 5 or Figure 6 with the voltage multiplied by the same factor that relates the full-scale voltages. The curves are based on 10V full scale.

Signals on the jacks on the rear panel of the optics assembly are related to gas concentrations by the calibration curves in Figures 5 and 6. These jacks may be connected directly to a recorder or meter if the digital assembly is not being used.

55<

Span Calibration Adjustments

Span calibration is related to the change in output signal due to the addition to the sample cell of a known concentration of CO or CO_2. The change is measured from the zero setting, which is the signal level observed with no absorbing gas in the sample cell.

At the time the monitor was shipped to Aerochem, the span calibration was properly adjusted on all 3 ranges (1, 5 and 20 ppm) of both channels (CO and CO_2). The estimated error in the calibration of the CO channel is the greater of 2% of the reading or 0.05 ppm. The corresponding numbers for CO_2 are 2% and 0.02 ppm. Monitors of this type normally display very stable span calibration and few adjustments are required. In the case that careful testing indicates that minor adjustments are required, they should be made with the span controls according to the following discussion.

The "master span" potentiometer on the main electronics card (see Figure 11) is used to change the sensitivity of all three ranges of one of the channels by exactly the same factor. A change in this potentiometer has the effect of shifting all 3 curves of either Figure 5 or Figure 6 upward or downward by the same distance on the logarithmic scale. Individual potentiometers mounted on the range card make it possible to change the sensitivity of a single range (1, 5, or 20 ppm) on either of the channels. These potentiometers are adjusted with a small screwdriver and are located above the main electronic cards near the top of the opening made by opening the hinged panel. The 3 potentiometers for each channel (CO_2 or CO) are labeled and correspond from left to right to the three ranges of sensitivity (1, 5 and 20 ppm).

The digital assembly has been programmed to give the proper relationships between voltages and concentration readings on the digital meters. These relationships cannot be changed without returning the digital assembly to Ford Aerospace.

Time Constant Switch

The time constant switch is located on the main electronics card for each channel. Time constants of 0.1, 0.3, 1, 3 and 10 seconds are available; the same value should be used for both channels.

Input Potentiometer

This potentiometer is located in the upper left-hand corner of the main electronics card. It is labeled "R1 INPUT" in Figure 11 and is adjusted, if necessary, to maintain the input signal at approximately 45 meter units when the sample cells are filled with zero-gas.

NORMAL OPERATION

Checking Signal Levels

When first starting to operate the monitor, the signal levels should be checked with the sample cells and GFC enclosure flushed and with the monitor warmed up for approximately 2 hours or more. The normal operating values are given by the following table.

TABLE 1. NORMAL SIGNAL LEVELS

Meter Function	Signal Levels (meter units) Safe operating range -		setting when shipped	
	CO_2	CO	CO_2	CO
Reference	30-80	30-80	55	44
Signal Input	35-55	60-85	45	75
Carrier	52-56	47-51	54	49

There is little reason for the reference signal to change significantly from the value indicated in the table; small changes will not affect the performance of the monitor as long as the level is between 30 and 80 meter units. Carrier levels are determined by the permanent setting of the automatic gain control circuit. If this circuit is operating properly, the carrier level will be very near to the tabulated value as long as the input signal is between approximately 18 and 100 meter units. For best operation the input signal level should be 35-55 for CO_2 and 60-85 for CO. The input potentiometer may be used to adjust this signal to its appropriate value. If the gain must be increased significantly by adjusting the potentiometer, it may be an indication of misalignment of the optics or of improper cooling of the detector.

Gas Handling

The zero-gas line and sample-gas lines should be connected as discussed above, and the GFC enclosure should be flushed at approximately 0.5-1 liter per minute. Excessive flushing may cool the radiant energy source and cause noise on the output signal. If the flushing is too slow, the zero-setting may shift if the flushing rate is varied or if a person exhales near a ventilating inlet. The high concentration of CO_2 in the exhaled air can leak into the GFC enclosure and cause the shift.

The optimum flushing rates for the sample gases depend on the maximum amount of gas available from the catalytic oxidizer system and on the required sample turnover time. The relative flushing rates through the

two sample cells should be approximately in proportion to their volumes in order that the residence time of the gas is the same in both sample cells. It may be necessary to add some volume in the gas line of one of the channels in order to match simultaneously the resident times and the delay times. The delay time for each channel is the time required for a small volume of gas to move from the inlet of the CO_2 scrubber to the entrance to the sample cell.

It is recommended that the gas lines be heated so that the gases entering the sample cells are within $\pm$ 5°C of the 45°C sample cells.

MAINTENANCE AND TROUBLE SHOOTING

The monitor should require very little maintenance. This subsection gives a discussion of procedures to check for proper operation and for trouble shooting. The most likely problems are the burning out of the radiation source and misalignment of optics due to mishandling. Procedures for replacing the source are given below. Realignment of the optics should not be attempted without consulting Ford Aerospace engineers.

Replacing Radiation Source

The radiation source is a wire-wound resistor (Dale, 4.7 ohm, type G-3-72), 0.078" diameter by 0.40" long. To gain access to the source, remove the top cover of the rear portion of the optics assembly. The source is mounted on a small aluminum plate that forms part of the rear side of the GFC enclosure. The source protrudes inward from the plate and is removed with it. Electrical leads to the source can be disconnected at the terminal strip. Electrical continuity of the source can be checked without removing it. Before removing the source, it is necessary to remove the insulation and some of the silicone rubber sealant that seals the joints of the GFC enclosure.

A burned-out source can be replaced by one of the spares provided with the monitor. The leads on the resistor must be bent approximately the same as the ones on the resistor being replaced. When the mounted source is being reinstalled into the GFC enclosure, the mount should be adjusted carefully in the direction parallel to the motor shaft to produce maximum input signal in the CO channel. After the source has been replaced, the joints and the holes through which the electrical leads pass must be sealed.

Decrease in Detector Signal

Decreases in the input signal measured with the panel meter may be caused by several different problems including: burned-out source, misalignment of optics, dirt on the mirrors in the sample cells, improper cooling of the detectors, or malfunction of the preamplifier or main

electronics card. The input signal measured with the panel meter depends on the setting of the input potentiometer on the main electronics card, but the signal level at the output of the preamplifier is independent of this setting. This signal level can be observed easily with an oscilloscope. At the time the monitor was shipped to Aerochem, the peak-to-peak signal levels were 1.7 volts for the CO channel and 2.0-2.5 volts for the CO_2 channel.

The thermoelectric coolers for the two detectors are connected in series and draw approximately 1.3 amps. Fuse No. F5, located on the side panel, protects the coolers.

SECTION 7

ELECTRICAL CIRCUITS

Figure 8 is a schematic diagram of the 115 VAC power distribution circuits. The power switch and pilot lamp are located on the front panel. A Wanlass CLIP-AC regulates the voltage to provide better instrument stability. The enclosure for the GFC and the sample cells are temperature controlled. A 57-V transformer supplies power to the motor; operation at this reduced voltage greatly reduces the heat dissipated.

The main power fuse is located on the back panel. All other fuses are located on the side panel and are numbered as indicated in Figure 8.

Figure 9 shows the location of the heaters for the sample cells and the GFC enclosures. The lower portion of the figure shows the approximate positions of thermocouple junctions that can be used to monitor the temperatures at different locations. All of the thermocouple wires are connected to a terminal strip that is mounted on the shelf directly above the sample cells. The terminals are accessed by removing the top cover from the rear portion of the optics assembly.

60<

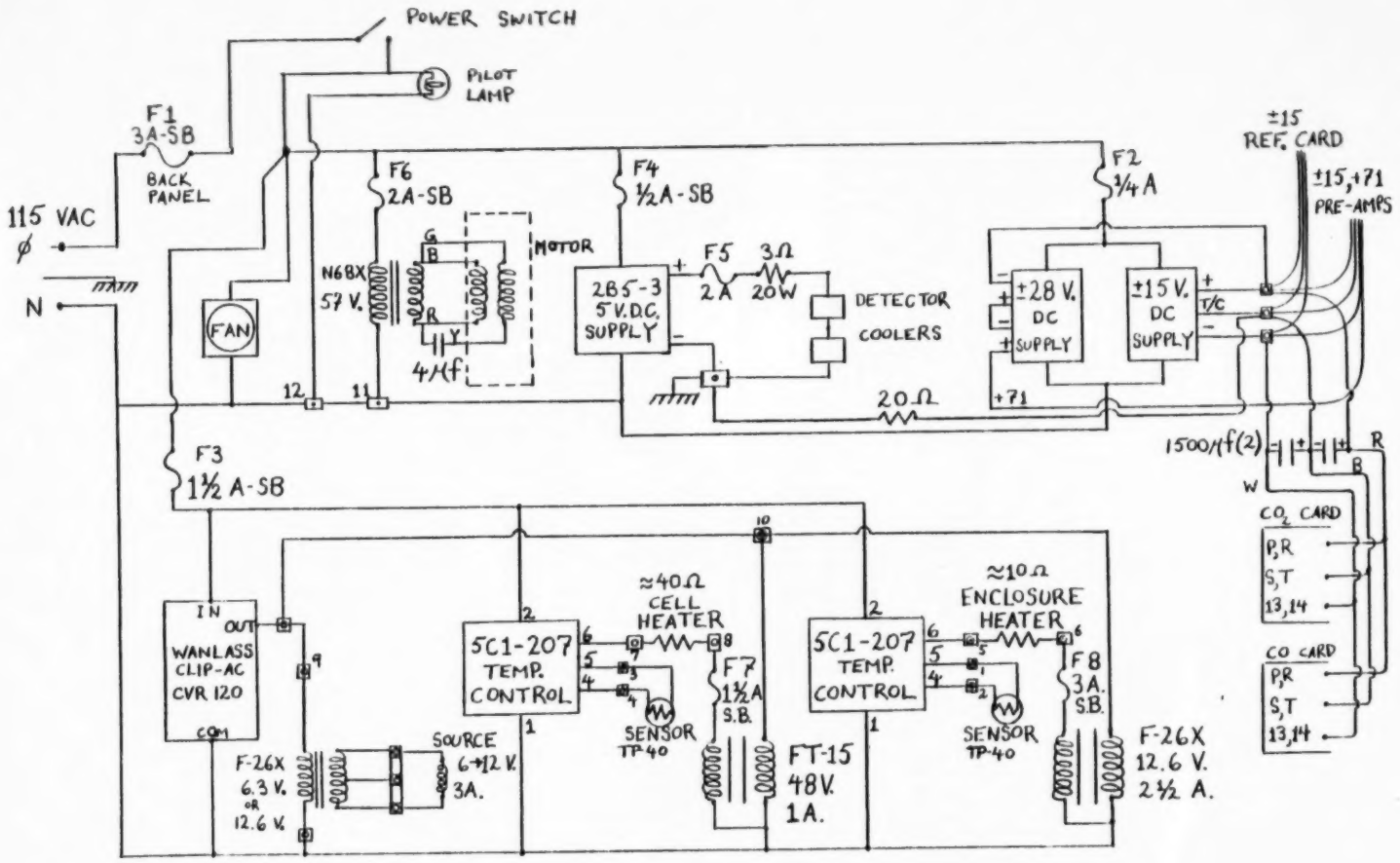

Figure 8. Electrical power distribution circuits.

POWER RESISTOR LOCATIONS

RESISTOR NO.	OHMS
①	3
②	6.8
③	2
④	27.3*
⑤	5
⑥	2
⑦	5.3
⑧	3.5

*HEATER WIRE 2 Ω/FT

CELL HEATERS

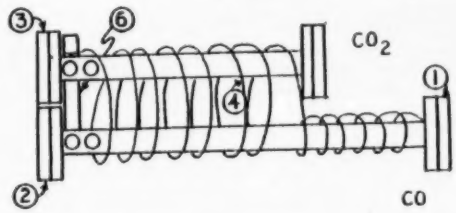

⑤ IN GAS LINE CONNECTING BULKHEAD

ENCLOSURE HEATERS

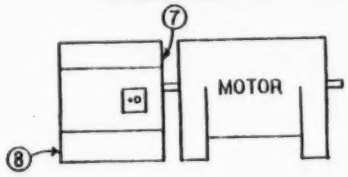

THERMOCOUPLE TERMINALS

TERMINAL #	LOCATED NEAR	
1	①	CELL HEATERS
2	②	
3	③	
4	④	
5	COMMON	
6	⑦	ENCLOSURE HEATERS
7	⑧	

Figure 9. Locations of heating resistors and thermocouples. All thermocouples are made up of copper-constantan junctions.

62<

SECTION 8
ELECTRONIC CIRCUITS OF OPTICS ASSEMBLY

A block diagram of the electronics that process the detector signals is shown in Figure 4. This section describes these electronic circuits in more detail. Most of the circuitry is contained on printed circuit cards. A single reference card serves both the CO_2 and CO channels; each channel has its own preamplifier card, main electronics card, and range card.

MAIN ELECTRONICS CARD

The two main electronics cards are accessed by opening the hinged front panel. The CO card is behind the CO_2 card, but all of the components that are adjusted during minor maintenance are available from the front or by a screwdriver through holes in the side of the monitor. A main card is illustrated in Figures 10 and 11 .

The main electronics card can be subdivided into three major systems: the 360-Hz carrier amplifier and demodulator system, the 30-Hz signal amplifier and demodulator system, and the 30-Hz reference system. The following text describes the adjustment of the controls mounted on the main electronics card and those mounted on the front panel. A short description is also given of the amplifier stages contained on the card.

360-Hz Carrier Amplifier and Demodulator

The gain of the preamplifier was adjusted with R_G (Fig 13) such that the 360 Hz carrier amplifier system was operating on signals that were at an optimum voltage. This adjustment was made with a new source of radiant energy in the optics system, clean windows in the sample cells, and the signal input potentiometer set near the middle of its adjustment range. The signal input potentiometer is adjusted as necessary to maintain the signal level within the operating range of the carrier system.

Stage AR1 (Fig 10) is a high-pass amplifier with a gain of 3 at 360 Hz and a pole at 16 Hz. The input level adjustment potentiometer R1 is set such that the input signal level is within the correct operating range for the card. The output of AR1 will be about 2 volts peak-to-peak when R1 is correctly set. R1 is normally adjusted such that the front panel meter reads approximately 45 units. If the input signal level is not between 35 and 50 units, non-linearities in the AGC can cause small output errors if the signal level varies.

Stage AR2 is an automatic gain-controlled stage that maintains the average demodulated carrier level constant at about -1.4 V as measured at the output of AR4. The output of AR2 is held at about 4.4 volts peak-to-peak. The stage consists of an inverting operational amplifier with FET Q1 acting as a variable attenuator with resistors R5 and R6. The impedence

at the drain of Q1 is proportional to the negative voltage at the gate. The impedance of Q1 is typically about 400 Ω. The voltage at the gate of Q1 is dependent on the average carrier level. Stages AR2 through AR5 are a closed loop AGC system. The AGC loop has a time constant of 1 second. Stage AR5 compares the average carrier level with the 1.4 volt reference voltage that is derived from the 15 volt supply voltage. AR5 then adjusts the gate voltage of Q1 as necessary to make the average carrier level equal to the reference voltage.

The AGC can be disabled by placing a jumper between test points B and D. Stage AR2 will have a fixed gain of 9. Placing a 20K multiturn variable resistor between test points A and C allows the gain of stage AR2 to be varied from about 0.5 to 8.5. These test points are available on pins 1, 2, 3, and 6 of the DIP socket on the card for test points A, B, D, and C, respectively. Pin 7 of the socket is at ±15 volts. It may be useful to disable the AGC to locate and correct a system malfunction.

Signal input levels that fall below 18 meter units, as indicated by the front panel meter, are outside of the range of the AGC. This 18 meter unit level corresponds to 30 to 50 percent of the optimum operating level, depending upon the instrument selected.

Amplifiers AR3 and AR4 comprise a precision full-wave demodulator with unity gain. The stage has a high-pass pole at 45 Hz.

30-Hz Reference System and Output Zero Control

Stage AR15 (Fig 10) shifts the phase of the 30-Hz reference signal over about a 160 degree range as phase potentiometer R73 is adjusted throughout its range. Stage AR16 is a differential comparator that converts the sinusoidal reference signal into a square-wave reference signal. The input and output of AR15 is a 2 volt peak-to-peak sine wave. The output of Stage AR16 is a 28 volt peak-to-peak square wave at the reference frequency. The output of Stage AR16 drives the gate of field-effect transistor Q3 in a switching mode of operation. Stages AR15 and AR16 are used for phasing and driving the 30-Hz synchronous demodulator, Stage AR10.

Stages AR17 and AR18 are similar to Stages AR15 and AR16 and are used to synchronously modulate the 360-Hz carrier at the 30-Hz signal frequency. This modulation occurs between Stages AR2 and AR3. The controls associated with Stages AR17 and AR18 are entitled zero Ø and zero switch. The phase (Ø) control, R79, on the circuit card is adjusted to make the modulation placed on the carrier by transistor Q2 driven by Stage AR18 agree in phase with modulation placed on the carrier by the gas being detected by the photodetector system. The front panel zero switch is used in combination with the front panel zero amplitude control to cancel any residual modulation on the carrier when no absorbing gas is present in the sample cell. The zero switch effects a 180° phase shift in the zero correction modulation as it is switched from the - to the + position. When the zero switch is in the off position, the zero control is inoperative. Stage AR19 is used to cancel any

quadrature phase signal component of modulation that is on the carrier. This component results from irregularities in the transmission of the rotating correlation cell that occur during fabrication of the unit. The input of the stage is a fixed 90° phase shifter. The output is an adjustable-amplitude square wave. A small portion of this square wave reference signal is summed with the demodulated carrier signal at Stage AR4. No quadrature correction is required for either of the main cards in the monitor described herein; therefore, the gain of the quadrature correction circuits has been turned to zero.

30-Hz Signal System

The output of Stage AR4 is a 360-Hz carrier that has been full-wave demodulated. The 30-Hz modulation that was imposed on the carrier by the photodetector rides on top of the demodulated carrier. If the demodulated carrier is observed with an oscilloscope, and a large 30-Hz signal is present, the wave form will be a full-wave demodulated 360-Hz signal that is modulated at 30-Hz. The 720-Hz ripple due to the carrier demodulation process is removed from the 30-Hz signal by a 3-stage RC filter at the input to Stage AR6. The output of Stage AR6 is a 30-Hz signal that is proportional to the amount of 30-Hz modulation that was on the carrier. The carrier is no longer present at this point. Stage AR6 is a buffer amplifier that drives the range span potentiometers that are mounted on the range card that is mounted on the front panel of the instrument.

Stage AR7 is a variable-gain wideband amplifier that can be adjusted for gains between 1 and 5 with span potentiometer R35A. This span adjustment changes all ranges by the same multiplicative factor. Stage AR8 is a 30-Hz tuned amplifier with a Q of 4.5 and a gain of 20. Stage AR9 is a bandpass amplifier with poles at 13 and 66-Hz and a gain of 14 at 30 Hz. Stage AR10 is a fullwave synchronous demodulator that operates at 30 Hz. The phase of the demodulator is adjusted with Stage AR15. Stage AR10 incorporates a low-pass filter with poles at 3 Hz and 30 Hz. The amplifier has a dc gain of 10 and has unity gain for frequencies above about 60 Hz. Stage AR11 is a dc-coupled differential amplifier that drives the time constant system, and was originally designed to subtract a water-correction signal from the main signal. The water-correction circuits are not used in the CO_2-CO monitor, because of the expected low concentration of water vapor in the samples.

Trim potentiometer R54 entitled "zero offset" is used to null any dc zero errors in stages AR10 through AR12. This adjustment should not be required unless components in these stages are changed. Stage AR12 is a high impedence buffer amplifier that allows the time constant switch to be switched without discharging the time constant capacitor C35. Stage AR12 is also a variable gain amplifier that can be adjusted for gains between 1 and 15. The time constant switch affords time constants of 0.1, 0.3, 1, 3, and 10 seconds. It is possible to charge the time constant capacitor on a fast time constant and then to switch to a long time constant if one wishes to speed up the time between readings. Time constant capacitor C35 is out of the circuit when the switch SW2 is in the 0.1-second time constant position. This time constant

approximates the measured response time of the system. The combined effects of the low-pass filters on stages AR10 through AR12 would result in a time constant of 0.07 seconds. The output of Stage AR12 can be applied to strip-chart recorders through either a fixed output jack (on the rear panel of the optics unit) on which the full output voltage of Stage AR12 is applied to the recorder, or by the variable-output jack (on the front panel) where any full-scale voltage between one millivolt and 10 volts can be implemented by adjustment of the recorder potentiometer R69 and the recorder level switch SW3. These adjustments do not affect the signal on the fixed output jack or on the panel meter.

Stage AR20 is a half-wave demodulator employed to rectify the input signal or the 30-Hz reference signal so that either can be displayed on the front panel meter. It also inverts the carrier level for display on the front panel meter.

REFERENCE CARD

A single reference card is used to supply a 30 Hz reference signal to the main electronics card. A schematic diagram of this card is shown in Figure 12. Amplifier AR1 of the reference card is a variable gain amplifier that can be adjusted for gains between 0.05 and 5. The second amplifier on the card is a 30 Hz tuned amplifier with a gain of 20 and a Q of 4.5 that is employed to convert the square wave output of the reference pickup into a sine wave suitable for use by the main electronics card. The potentiometer on the reference card is adjusted to give approximately a 2 volt peak-to-peak output sine wave at the 30 Hz reference frequency. The adjustment is stable and should not require readjustment unless a component is changed or the reference pickup decreases its output with age. All adjustments have been preset before the instrument was shipped. The output of the 30 Hz reference card is displayed on the front panel meter when the meter switch on the main card is in the reference position. A properly adjusted reference will indicate 50 ± 5 units on the front panel meter.

PREAMPLIFIER

Two preamplifiers can be contained on each preamplifier card. The preamplifier is a bandpass amplifier with poles at about 3 Hz and 1500 Hz. The gain of a preamplifier is adjusted to match the photodetector to the channel with which it is used. The preamplifier gain is adjusted by selecting resistor R_G such that the preamplifier voltage is between 0.8 and 1.2 volts peak when the system is operating with a new source and clean windows. A preamplifier card is illustrated in Figure 13.

RANGE CARD

Figure 14 illustrates the range card. It is located behind the hinged front panel, just above the main electronics cards. This card contains two adjustable attenuators for each of the three ranges of the instrument. The front panel range switch selects the appropriate attenuators (one for the CO_2 channel, one for the CO channel) for the gas concentration being measured.

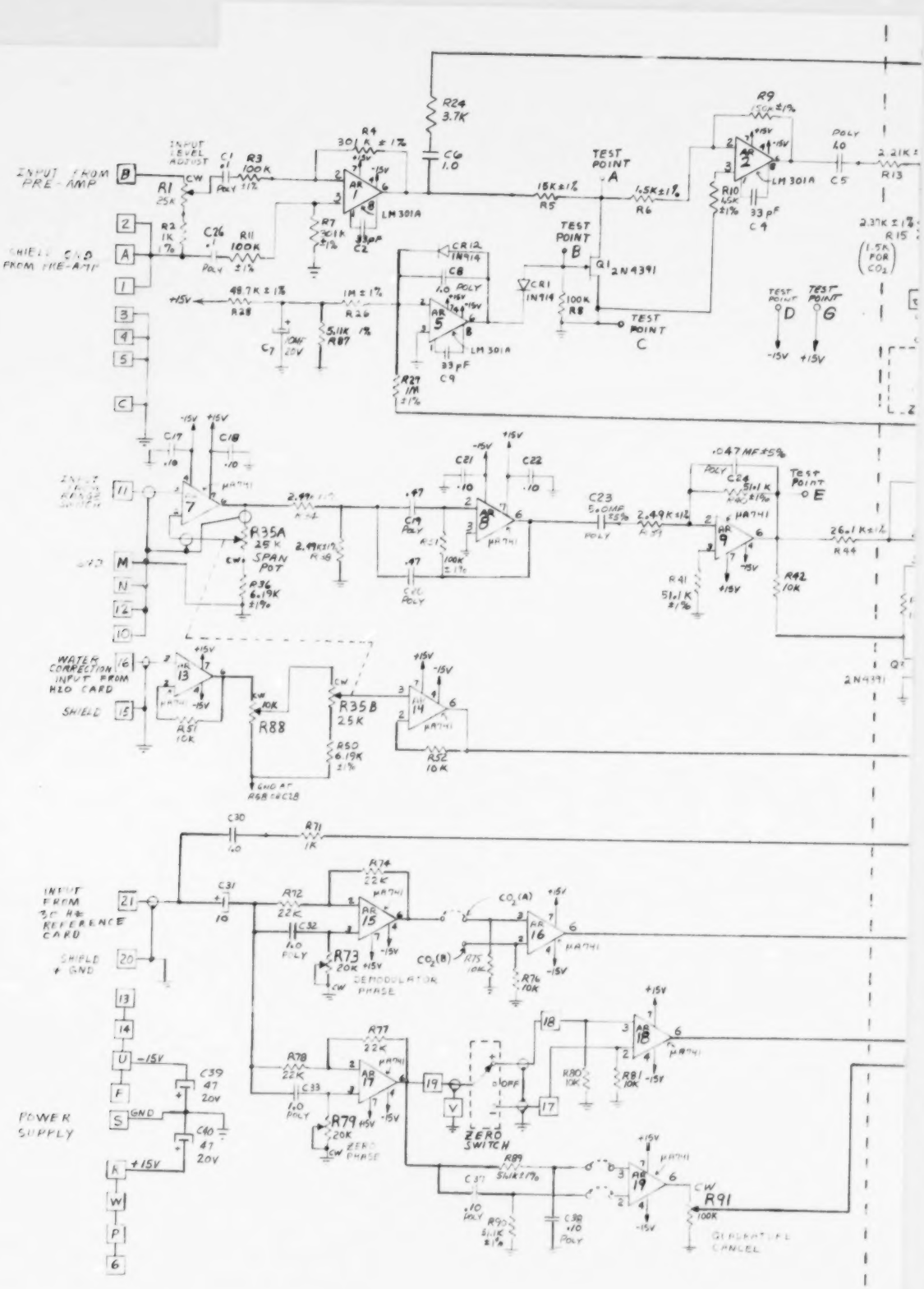

Figure 10. Schematic diagram of the main electronics card. Schematic is continued on the following page.

67<

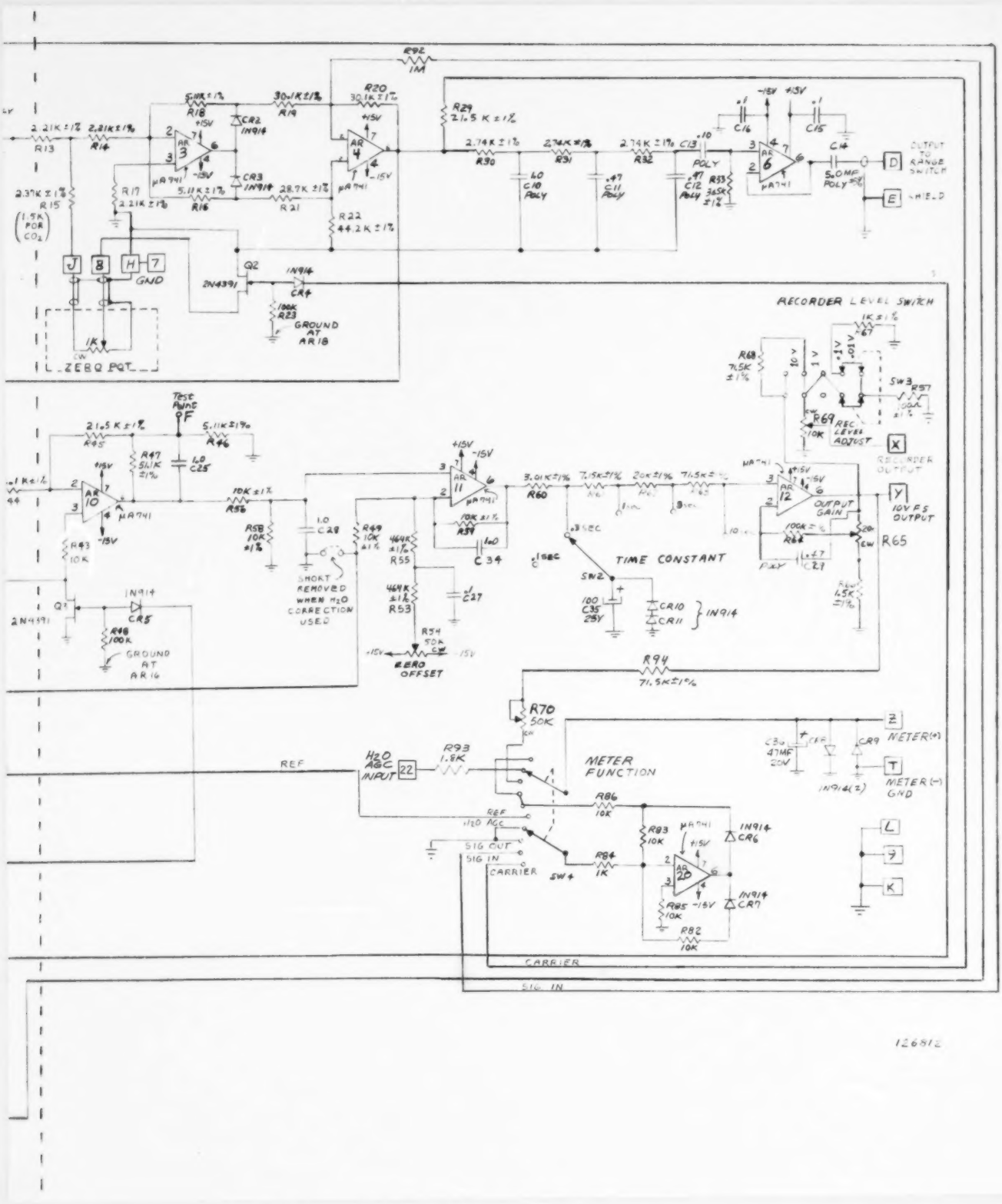
RECORDER LEVEL SWITCH
TIME CONSTANT
ZERO OFFSET
METER FUNCTION
OUTPUT GAIN
REC LEVEL ADJUST
GROUND AT AR16
GROUND AT AR18
SHORT REMOVED WHEN H2O CORRECTION USED
OUTPUT TO RANGE SWITCH
SHIELD
10V F.S. OUTPUT
METER (+)
METER (-)
GND
H2O AGC INPUT
REF
SIG OUT
SIG IN
CARRIER
ZERO ADJUST

Signals from Stage AR6 on the main cards are attenuated in a 1,.24,.1 sequence for CO_2 and a 1,.2,.06 sequence for CO as the range switch is switched through the 1, 5, and 20 ppm ranges respectively. These 30 Hz signals are then returned to Stage AR7 of the main cards for further processing.

In addition, a four pin connector on the back of the CO_2-CO monitor is wired to the range switch such that pin 4 is shorted to pins 1, 2, and 3 as the range switch is switched through the 1, 5, and 20 ppm positions respectively. This provides a digital low for the analog-to-digital amplifier assembly so that the non-linear output corresponding to each concentration range can be applied to the particular seventh order polynomial that will generate a linear read-out.

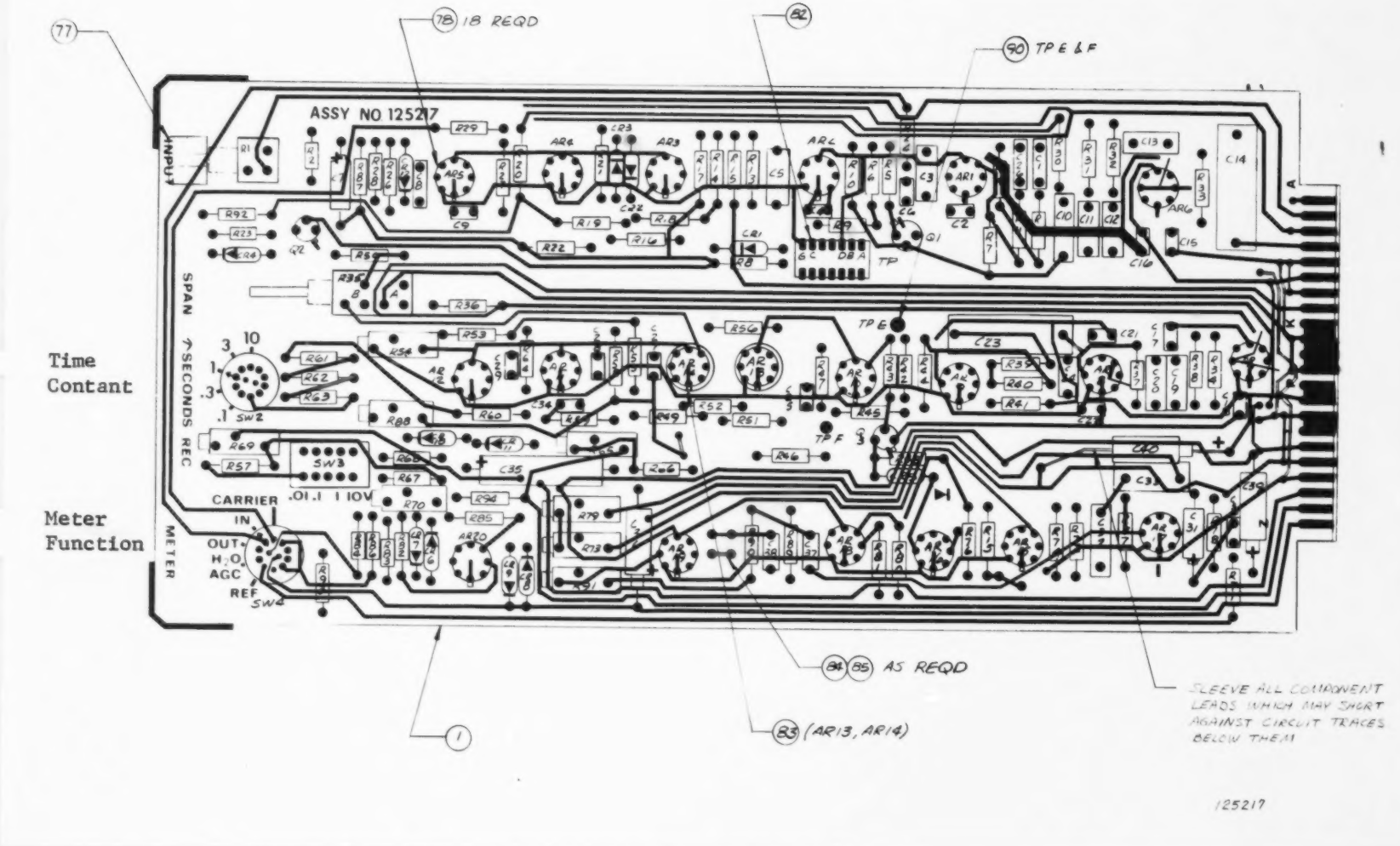

Figure 11. Assembly drawing of the main electronics card.

NOTES: UNLESS OTHERWISE SPECIFIED

1. ALL RESISTORS ±5% 1/4 W
2. ALL 1% RESISTORS RNC65J TYPE

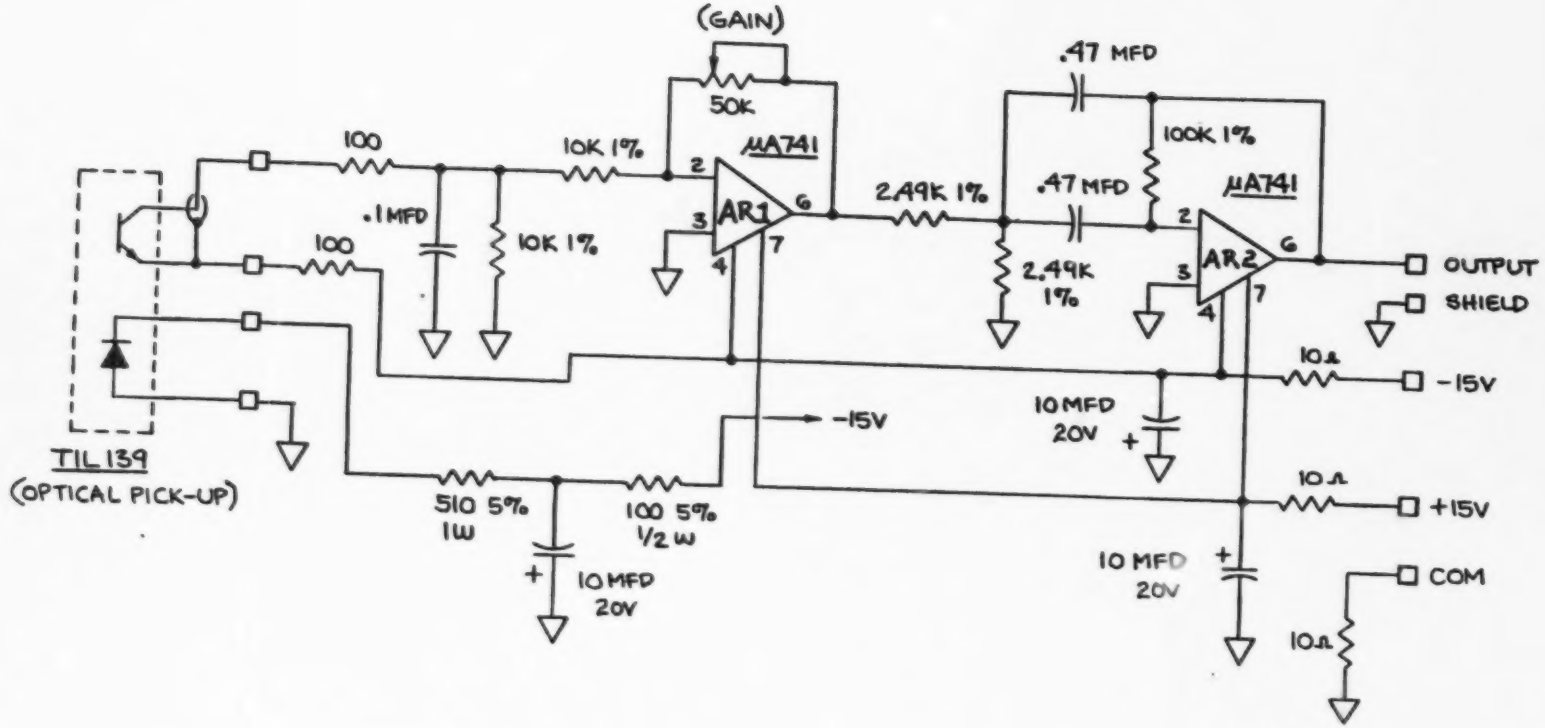

Figure 12. Circuit diagram of the 30-Hz reference card.

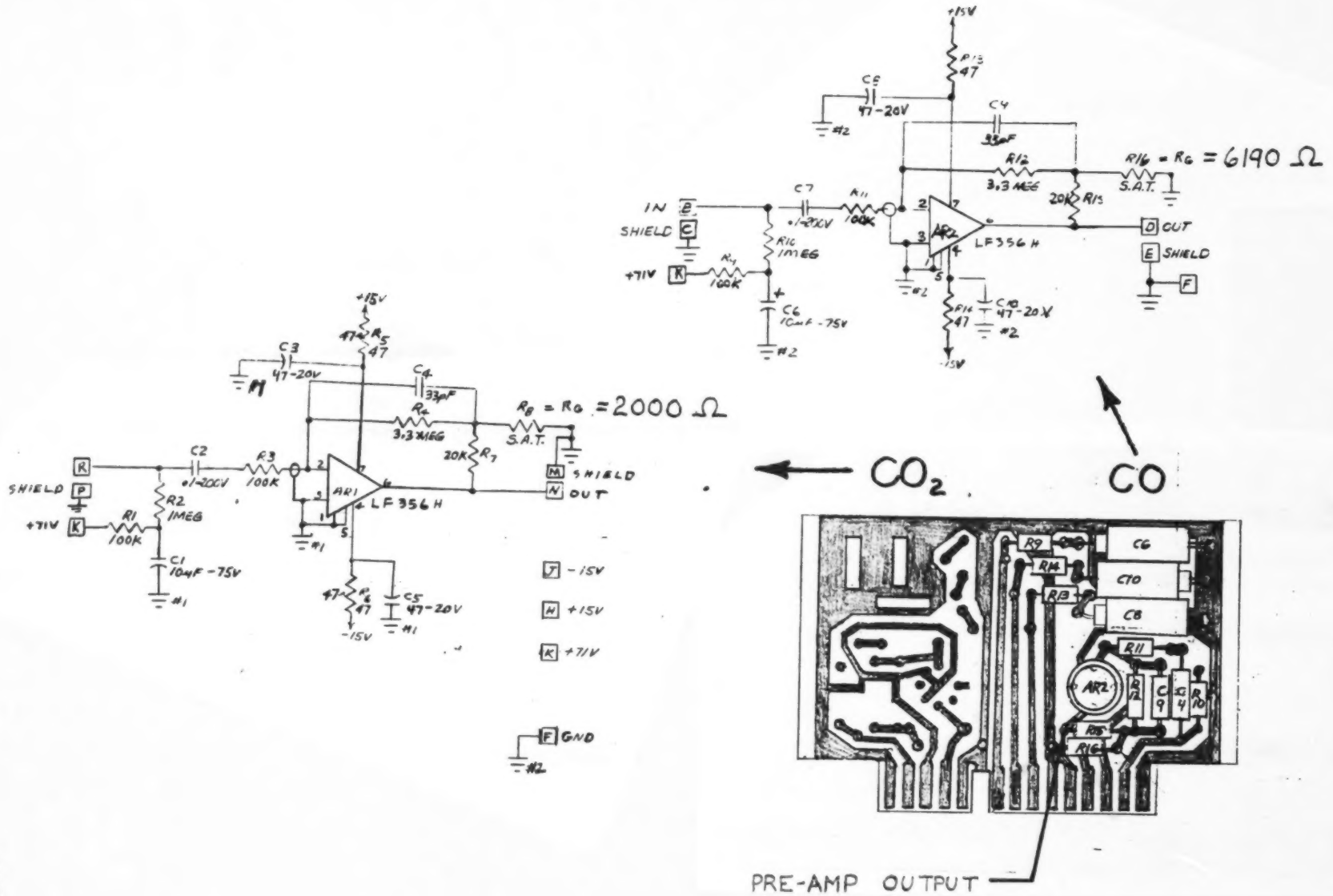

Figure 13. Detector preamplifier circuit. The preamplifier output test points are indicated on the card.

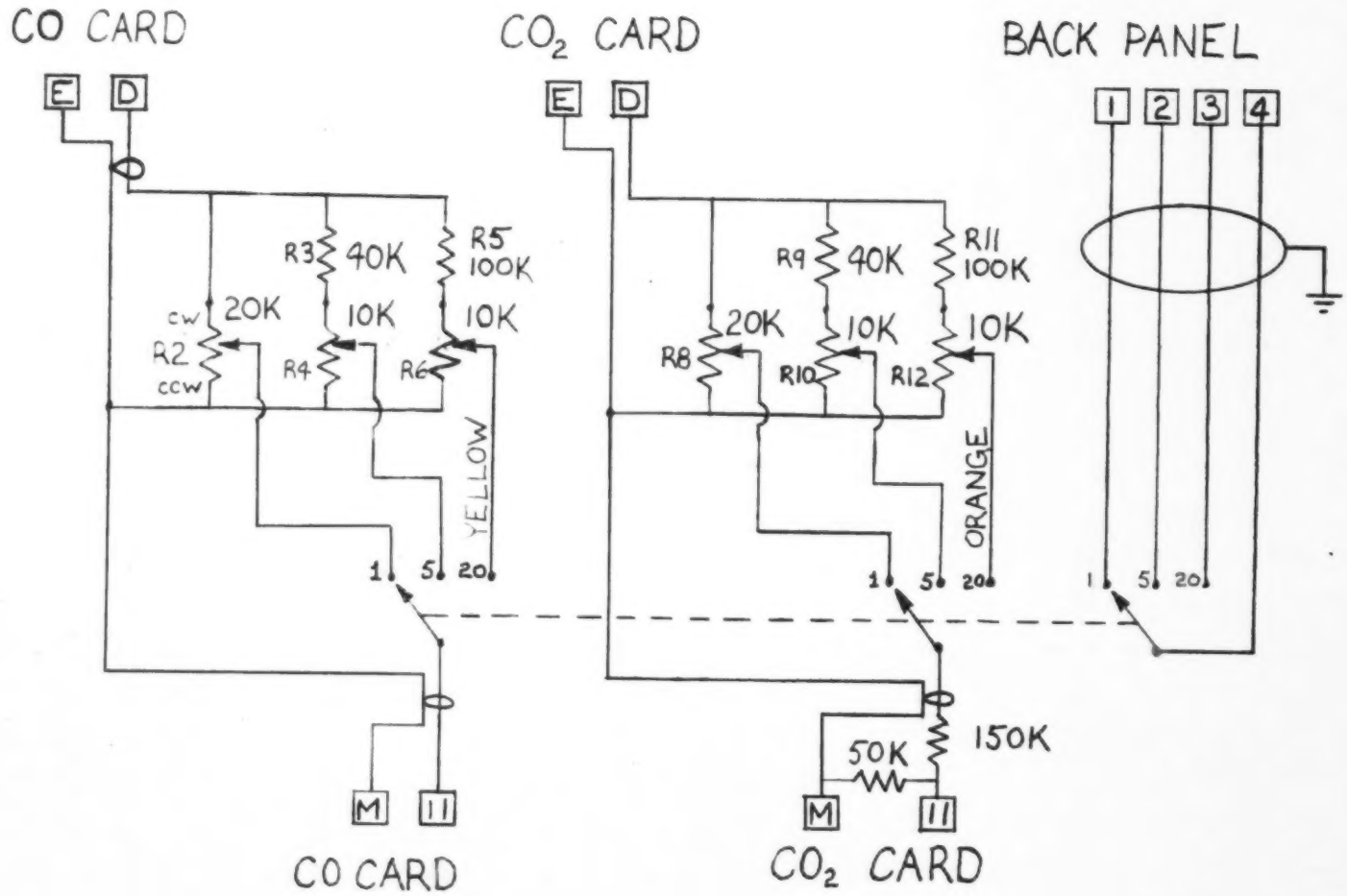

Figure 14. Circuit diagram of the range card.

SECTION 9

DIGITAL PROCESSOR ASSEMBLY

The EPAGAM digital processor (DP) contains three commercially available logic/signal processing boards: (1) MSC8001 CPU, (2) RTI 1202 A/D, and (3) RTI 1201 D/A. These boards are housed in a National Computer chassis model RM655.

The digital processor receives from the optical assembly the two analog output signals (one each for CO and CO_2) that are related non-linearly to the gas concentrations. The processor then accounts for the non-linearities and provides two output readings for each gas; one is a digital readout in ppm, and the other is an analog signal that is directly proportional to the gas concentration. A corresponding pair of readings is also provided for the difference (CO_2 - CO) between the concentrations of the two gases. This concentration difference is equal to the concentration (in ppm) of carbon atoms in the non-methane hydrocarbons in the gas sample entering the sample conditioner.

Analog voltages received by the digital processor from the optical assembly are converted into 12-bit digital words and are input to the CPU. The CPU processes these words and solves fourth-order polynomials to account for the non-linearities in the relationships between the analog voltages and gas concentrations. Coefficients for the polynomials were determined experimentally by measuring the output signals for a series of standard calibration gases with known concentrations of CO and CO_2. These coefficients reside as firmware in a PROM in the digital processor.

A simplified block diagram for the DP is shown in Figure 15, and the detailed interface between the optical assembly and DP is illustrated in Figure 16. In order to provide adequate resolution of concentration levels over a large dynamic range while using the limited $\pm$ 10v analog signal range, the concentration levels are divided into three ranges: 1 ppm, 5 ppm, and 20 ppm full scale. The range is selected by the operator and is controlled manually with the range switch on the optical assembly. A separate non-linear relationship exists between output voltage and gas concentration for each range setting. Therefore, the setting of the range switch determines which non-linear relationships are used to calculate the gas concentrations displayed on the LED readouts. As shown in Figure 15, the DP has three LED digital readouts that display the concentrations of CO_2, CO, and the difference (CO_2 - CO) between these concentrations.

The DP also provides the concentration levels as analog outputs through the A/D - D/A combination, as shown in Figure 15. The analog output of the digital processor for either channel is + 10v when the gas concentration equals the full-scale setting of the range switch on the optical assembly. As an example, if the CO concentration is 4 ppm, the analog signal is 8 v when the range switch is in the 5 ppm position and 2 v when the switch is in the 20 ppm position.

Also shown in Figure 15 is the optional printer interface. The CPU has the capability to interface with and control a column printer providing hard copy of the displayed concentration levels. This option may be added at any time by specifying the printer type/control interface and adding the appropriate software steps. Modifying the program requires detailed knowledge of the existing program and the capability to update the stored program in the PROM's.

The concentration levels displayed by the LED's are updated at approximately a 4-Hz rate. The sequence of events leading to a readout update is defined by tne flow chart in Figure 17.

Detailed information on the structure or operation of the CPU may be obtained from the MSC 8001 User's Manual available from Monolithic Systems, Inc., 14 Inverness Drive East, Englewood, Colorado 80112.

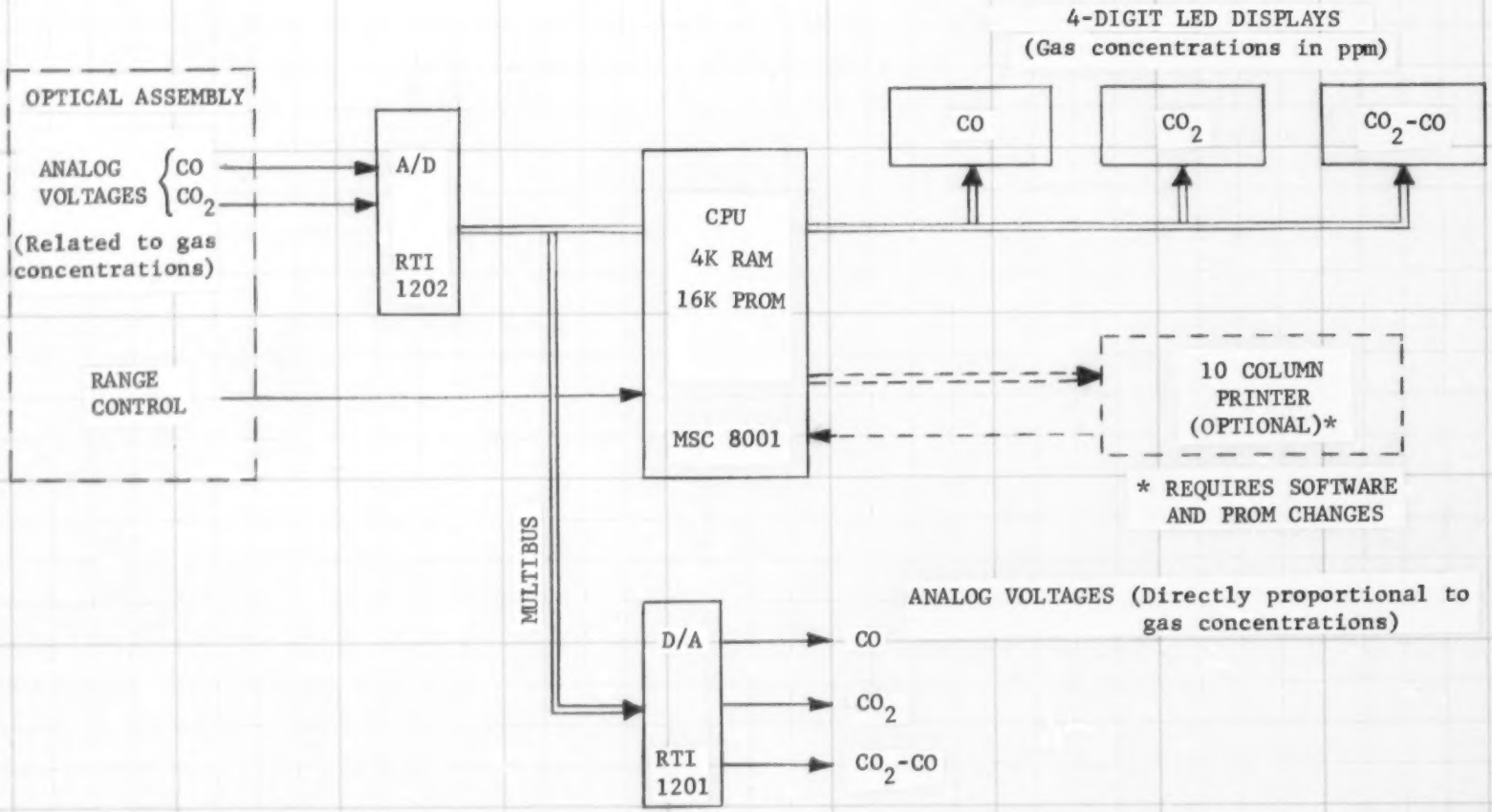

Figure 15. Simplified block diagram of the digital processor.

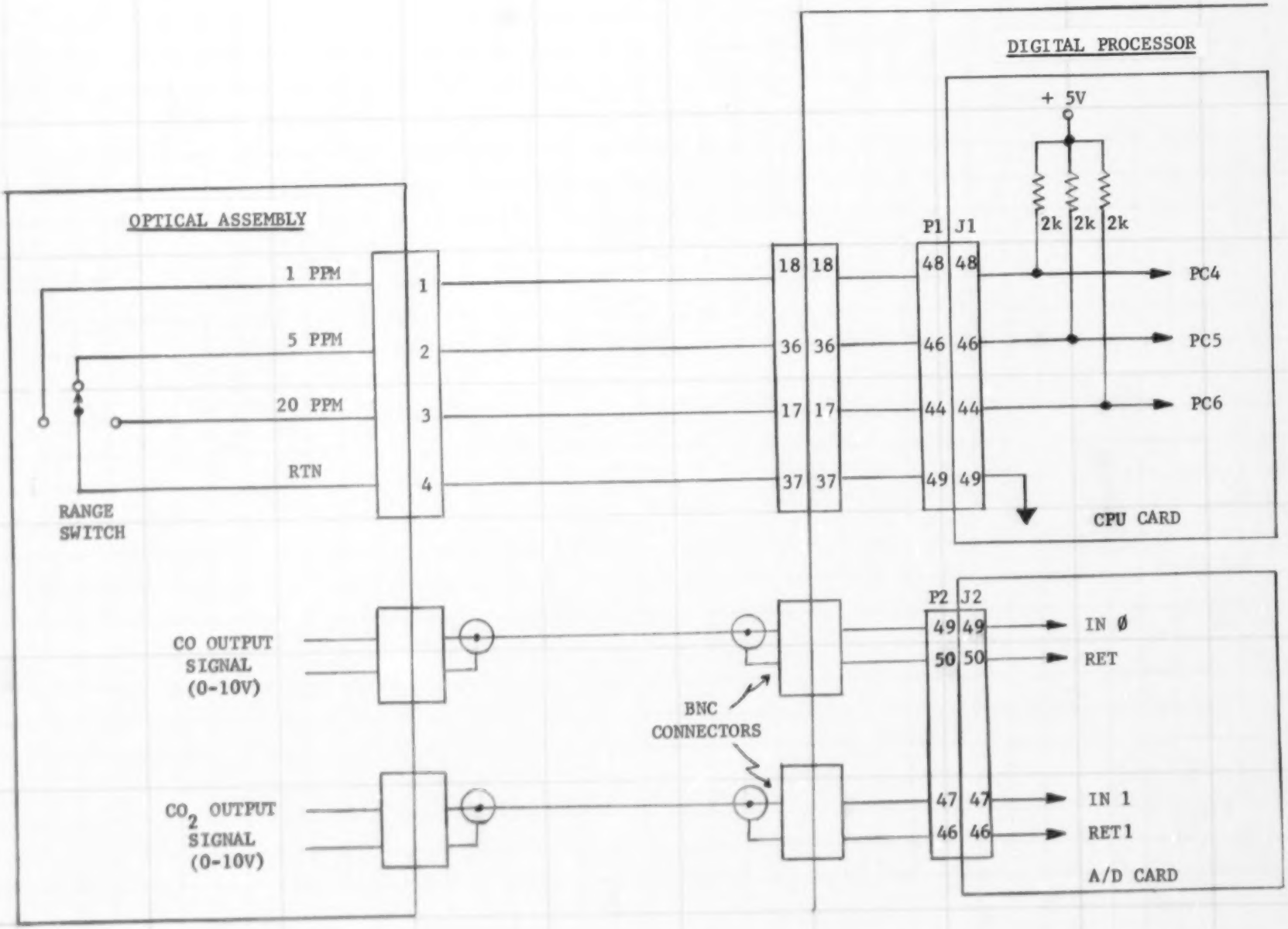

Figure 16. Electrical interface between optical assembly and digital processor.

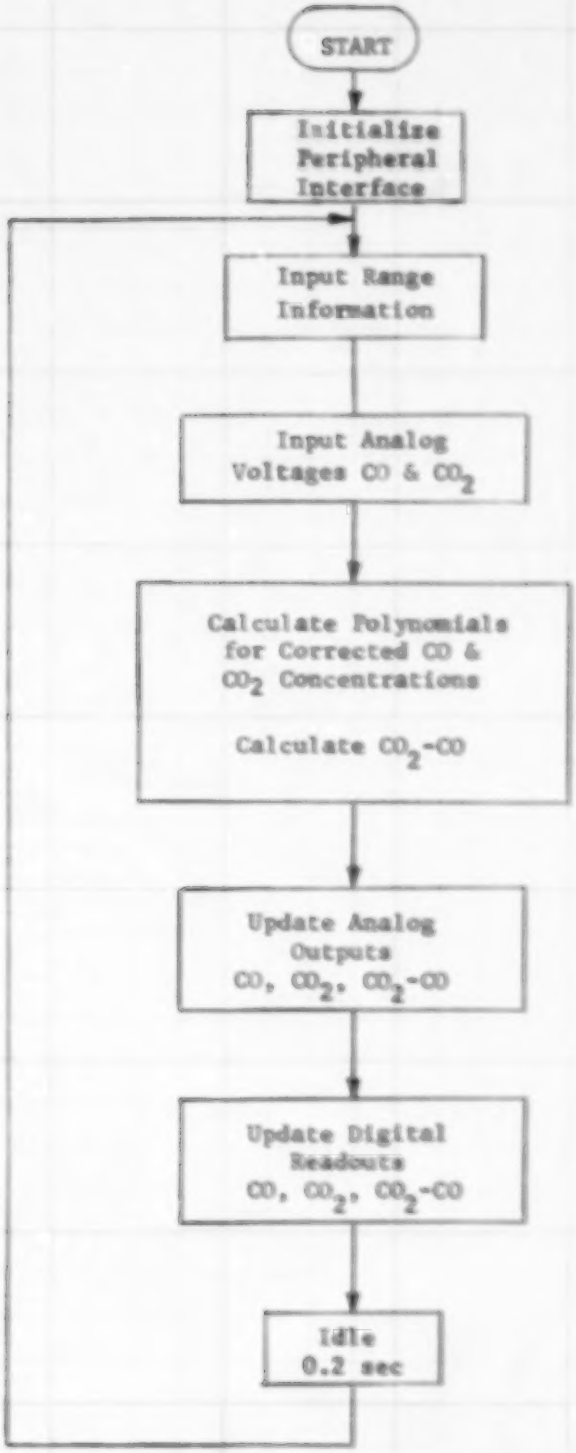
START
Initialize Peripheral Interface
Input Range Information
Input Analog Voltages CO & CO_2
Calculate Polynomials for Corrected CO & CO_2 Concentrations
Calculate CO_2-CO
Update Analog Outputs CO, CO_2, CO_2-CO
Update Digital Readouts CO, CO_2, CO_2-CO
Idle 0.2 sec

Figure 17. Data processor flow chart.